# FFI RAPPORT

## Friction Studies Related to Wear of Gun Barrels

Moxnes John F, Frøyland Øyvind

**FFI/RAPPORT-2005/01919**

# Friction Studies Related to Wear of Gun Barrels

Moxnes John F, Frøyland Øyvind

FFI/RAPPORT-2005/01919

**FORSVARETS FORSKNINGSINSTITUTT**
**Norwegian Defence Research Establishment**
P O Box 25, NO-2027 Kjeller, Norway

**FORSVARETS FORSKNINGSINSTITUTT (FFI)**
**Norwegian Defence Research Establishment**

**P O BOX 25**
**N0-2027 KJELLER, NORWAY**

**UNCLASSIFIED**

**SECURITY CLASSIFICATION OF THIS PAGE**
**(when data entered)**

**REPORT DOCUMENTATION PAGE**

| 1) PUBL/REPORT NUMBER | 2) SECURITY CLASSIFICATION | 3) NUMBER OF PAGES |
|---|---|---|
| FFI/RAPPORT-2005/01919 | UNCLASSIFIED | 48 |
| **1a) PROJECT REFERENCE** | **2a) DECLASSIFICATION/DOWNGRADING SCHEDULE** | |
| FFI-V/860/01 | - | |

**4) TITLE**

# Friction Studies Related to Wear of Gun Barrels

**5) NAMES OF AUTHOR(S) IN FULL (surname first)**
Moxnes John F, Frøyland Øyvind

**6) DISTRIBUTION STATEMENT**
Approved for public release. Distribution unlimited. (Offentlig tilgjengelig)

**7) INDEXING TERMS**

| IN ENGLISH: | IN NORWEGIAN: |
|---|---|
| a) Wear | a) Slitasje |
| b) Friction | b) Friksjon |
| c) Lands | c) Bommer |
| d) Grooves | d) Rifler |
| e) Gun barrel | e) Våpenrør |

**THESAURUS REFERENCE:**

**8) ABSTRACT**

In this article a study of the wear of the 12.7 mm gun barrel is performed. Two new measuring methods have been developed to study the wear rates. Electron probe microscopy was also used. Theoretical and experimental results are compared. We find that the heat flux into the lands of the gun barrel due to the mechanical friction force between the jacket of the projectile and the lands of the gun barrel is significant. The heat flux leads to a more brittle morphological structure of the steel in a region close to the surface of the lands. Increased brittleness is known to strongly enhance wear rates.

| 9) DATE | AUTHORIZED BY This page only | POSITION |
|---|---|---|
| 2005-12-10 | Bjarne Haugstad | Director of Research |

ISBN 82-464-0983-2

**UNCLASSIFIED**

**SECURITY CLASSIFICATION OF THIS PAGE**
**(when data entered)**

**CONTENTS**

Friction Studies Related to Wear of Gun Barrels

## 1 INTRODUCTION

Gun erosion has been known as an inevitable problem in use of current gun systems, although extensive efforts have been paid to minimize it. Gun erosion occurs as an increase in the bore diameter, allowing significant amounts of gas to escape past the projectile. Thus reducing muzzle velocity, muzzle range, muzzle accuracy and penetration due to increased yaw.

For tank guns, which need to be very accurate in order to hit a target, the permissible wear is about 1% of the bore diameter. For indirect fire weapons the allowable wear could be up to 10%. Typical wear rates vary between 0.1-200 microns pr round. As a rule the gun designer arranges for fatigue life of a barrel to exceed its wear because fatigue failure is usually catastrophic and endangers the gun crew. The normal situation is that maximum wear is situated at the commencement of the rifling of the bore. This is also the point at which the heat transfer from the hot propellant gas to the barrel surface is greatest (!). The bore temperature can reach 900-1500 K. Heat transfer may be 500 $MW/m^2$, and the propellant gas pressure may reach 600 MPa. The gun barrel gases consist mainly of CO, $H_2$, $CO_2$ $H_2O$ and $N_2$.

The leading parameter controlling the wear of the gun barrel surface is the maximum temperature of the gun barrel surface [1]. The wear is exponentially related to maximum temperature. The heat flux into the gun barrel surface is thus important to control.

In order to achieve significant wear the surface in the gun barrel either transforms to a more brittle steel material due to cycling temperature variations during a shot, or chemical reaction processes take place changing the gun barrel steel into more brittle materials as iron oxides or iron carbides. Also hydrogen embrittlement is believed to take place. The more brittle materials are more easily wiped off mechanically by the projectile or by the gun barrel gases. Increasing wear due to increased thermal stress also could be a significant factor. Also, the melting temperature of Iron Carbide is around 1200K, i.e. much lower than the meting temperature of steel (1800K).

If during firing gunpowder or gunpowder gases are able to move between the gun barrel and the projectile and finally ahead of the projectile, the gun barrel radius increases much more rapidly pr shot. The fluid mechanic situation is called scoring. It is believed that significant erosion due to scoring only appears at the terminal stage of the gun barrel lifetime. Scoring is sometimes causing significant melting of the gun barrel surface.

The heat flux into (positive) the gun barrel is due to four different mechanisms; a) the heat flux directly from the burning particles, which can have a higher temperature than the average gun powder gas temperature (flame temperature), b) the heat flux due to the hot gases with a

temperature equal to the flame temperature, c) the heat flux due to the exothermal chemical reaction during the oxidation/carburisation process, and finally d) the heat flux due to friction between the projectile and the gun barrel.

The situation in a) is very difficult to analyse and control since the main physics of this type of mechanism is difficult to establish. It is observed that when finely ground solid nitramines are used, the erosion is considerably less than when larger particles are used. One therefore believes that impingement of burning particles, which burn with higher flame temperature than of the average flame temperature of the gas, causes the increased erosion loss.

The situation in b) is more easily analysed by using ordinary fluid mechanic heat transfer theory. The heat transfer coefficient is increasing with the density, velocity and conductivity of the gunpowder gas, but decreasing with the viscosity. The composition of different species in the gunpowder gas is therefore indirectly affecting the erosion due to the varying heat transfer of the gases. Typically, hydrogen gas has high conductivity, and is accordingly believed to enlarge the heat transfer into the gun barrel. The heat flux due to chemical reactions (c) can be neglected since gunpowder only includes minor amounts of oxygen. The heat flux due to mechanical friction (d) is not usually studied, but will be the main objective in this article.

Thermal wear processes of steel alloys are classified into two main categories with respect to the magnitude of the heat flux. A) Melt and wipe off mechanism which occurs due to inert or reactive heating of the surface, leading to melting and subsequent removal of the melt layer, B) chemical mechanisms due to chemical interaction between reactive gun powder gases and the steel surface. The reacted zone is wiped off mechanically or by the aerodynamic forces. It the temperature is above the melting temperature both mechanisms contribute to the erosion process. For most practical problems only the mechanism B) is involved.

Greaves and co workers investigated the erosion of gun barrels [7]. They concluded that the erosion occurring in large guns was almost wholly due to the melting and sweeping away of metal from the bores surface by the rapid stream of highly heated propellant gas.

Evans and co-workers [8] made a comprehensive study of the chemical erosion of steel. They studied the erosive effects of high pressure and high temperature gases produced by the combustion of $CO/CO_2$ mixtures. They found that in general the erosion increased when the adiabatic flame temperature of the products increases and as the $CO_2$ concentration increases. They found erosion also when the temperature of the bore surface was below the melting temperature.

Four different approaches are experimentally handled in the literature to study the erosion process. One approach is to study the life times of gun barrels being in use [1]. A simple equation of the Arrhenius is derived that relates the wear pr round to the initial temperature, the maximum surface temperature and the erosivity of the propellant. The equation is verified by data on the wear rates of numerous gun and propellant combinations. It was found that CO and $H_2$ are very erosive. The problem with this approach is that a clear understanding of the different erosion mechanisms is difficult to achieve by using the aggregated analysis.

Another design is the vented vessel design ([1]-[3]). In this design hot gun barrel gas are allowed to leak out from a nearly closed combustion chamber to mimic the gas flow during a shot. The erosion is studied by using different materials in the vented region (erosion disk), and by creating different time histories of the pressure during venting of the vessel. Typically the amount of gunpowder and the orifice area of the combustion chamber are varied.

The interaction between the projectile and the gun barrel is not studied. Also, it is difficult to study the different gunpowder gases separately. In [2] two different thresholds were found experimentally. The first represent the onset of erosion and the second represent the transition from purely inert to inert plus reactive flow. The inert erosion was given by a pure wipe and wipe-off process. For a given free stream condition the onset of erosion depends on the geometry of the flow and the thermal properties of the substance under investigation. In [3] the temperature of the steel was lower than the melting temperature. It was found that the erosion was strongly controlled by the chemical interaction of the propellant gasses with the steel alloys. It was found that the erosion rate was dependent upon the thermal properties of the steel alloy. The higher the thermal conductivity of the alloy the lower the mass removal experienced by the alloy. Finally it was found that the erosion rate was linearly dependent of the number of firings in the vented chamber.

A third experimental design developed to study the erosion is the ballistic compressor [4]-[6]. The ballistic compressor utilizes a reservoir of driver gas to drive a piston to compress adiabatically the desired test gas. In this manner, the apparatus produces a quantity of hot, high–pressure gas that flows through the choked test orifice. Thus the problems associated with large number of gaseous species were overcome with this design. With the exception of the oxygen mixtures and hydrogen, the remaining test gases produced minimal mass removal. The results showed that the erosion of the steel alloys was controlled by surface chemical reactions of oxygen. The augmentations in erosion due to action of $H_2$ were attributed to the high diffusivity of $H_2$, which increases the surface heat transfer coefficient. For some oxygen concentrations the heat flux due to the exothermal chemical reaction was higher than the inert heat flux due to the gas stream. Reference [4] found that CO, $CO_2$ and $N_2$ mixtures gave insignificant erosion compared to mixtures of $O_2$ and $H_2$. Reference [6] states that results for high temperature corrosion under low flow conditions do not apply when very high shearing flows sweep away protective layers. In such cases the metal surface is exposed to heterogeneous chemical attack. They suggested that that water vapour could be the main erosion source in combustion gas atmospheres. They concluded that only the forward chemical reaction take place due to the wipe off of the FeO by the shearing forces.

A newer experimental design is to use laser pulse heating [12]-[15]. It was shown that the laser pulse heated specimen showed much of the same characteristic as the surface of a gun barrel. Of special interest in this study was the origin and loss of the protective chromium-coating layer.

Reference [9] examined the thermodynamic aspects related to steel reactive erosion. The temperature dependencies of the oxygen partial pressure and the carbon activity of the gas mixture as well as of main components of the steel alloy were calculated. It was shown that the thermodynamic approach could interpret various experimental results of steel erosion.

Some numerical codes have been developed to study gun barrel wear. In reference [10] a numerical model is devolved that tackles both thermal and chemical erosion of iron. It consists of a coupling between an interior ballistics code, which gives the history of the aerodynamic field, and an erosion code. The model explains the carburising/oxidation behaviour, and first validations with vented bomb data showed encouraging results. In reference [11] a unified computer model that predicts the thermochemical erosion in gun barrels is presented. The first two modus of the program include the interior ballistic code and the non-ideal gas thermochemical equilibrium code. The last three modules include a mass addition code, the gas wall chemistry code and the material ablation conduction erosion code.

Studies of real gun barrels show that the lands are worn faster than the grooves. This suggests that the interaction between the projectile and the gun barrel is important. Interestingly, the reasons for the increased wear of the lands are not provided by the literature. It is known from the vented vessel design and from studies of life times of gun barrel in use, that different gunpowders give quite different wear rates of the gun. This suggests that the heat flux due to friction between the projectile and the lands are small compared to the heat flux due to the gunpowder gases. It is not believed that the heat flux from the gunpowder gases is larger on the lands. Thus the larger wear of the lands is explained by larger mechanical wear in this region due to the stronger interaction between the projectile and the lands compared to the interaction with the grooves. The wear is induced by a homogeneous temperature enhancement in all regions along the surface of the lands and the grooves.

The final erosion approach studied in this article is to use a special experimental set up where the interaction between the projectile and the gun barrel surface is more easily studied. The design is constructed such that a short cylindrical part of the gun barrel can be taken out and studied. We used hardness measurements, metallography and Electron Probe Micro Analyser (EPMA) to study the wear of the gun barrel. We also measured the friction force between the projectile and the gun barrel with a special designed tool.

## 2 EXPERIMENTAL SET UP FOR WEAR STUDIES

The design of the gun barrel is constructed such that a short part of the gun barrel can be taken out for examination. This part is placed nearest the casing chamber where the wear is greatest. The calibre of the gun barrel is 12.7 mm.

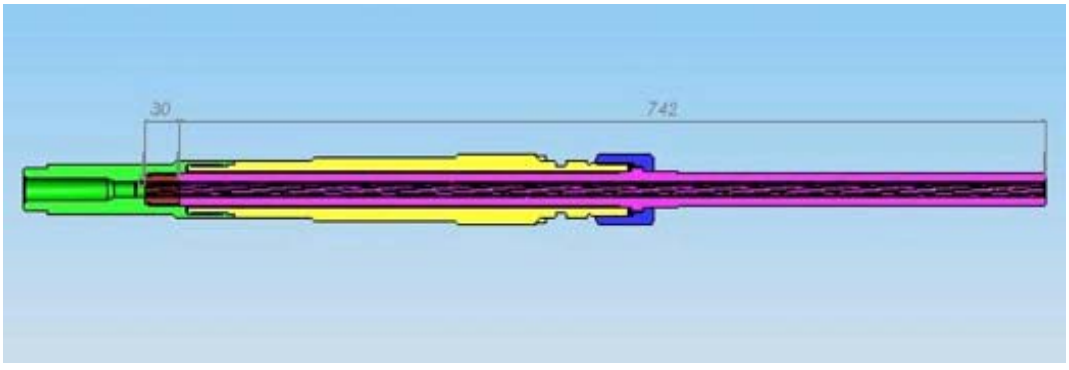


*Figure 2.1: The experimental gun barrel design.*

## 3 METALLOGRAPHIC STUDY

After 25 shots the wear of the gun barrel specimen is studied using different kinds of methods. Figure 3.1 show a close up of a gun barrel specimen. It also denotes the name of the different regions.

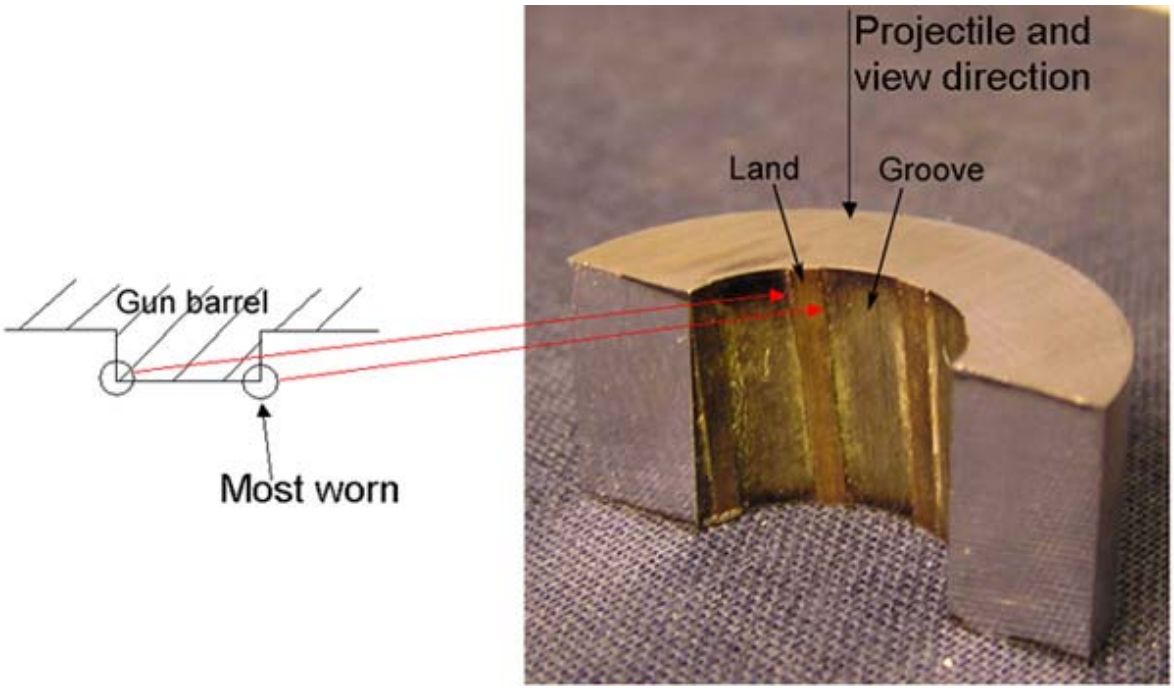


*Figure 3.1: Description of view of gun barrel.*

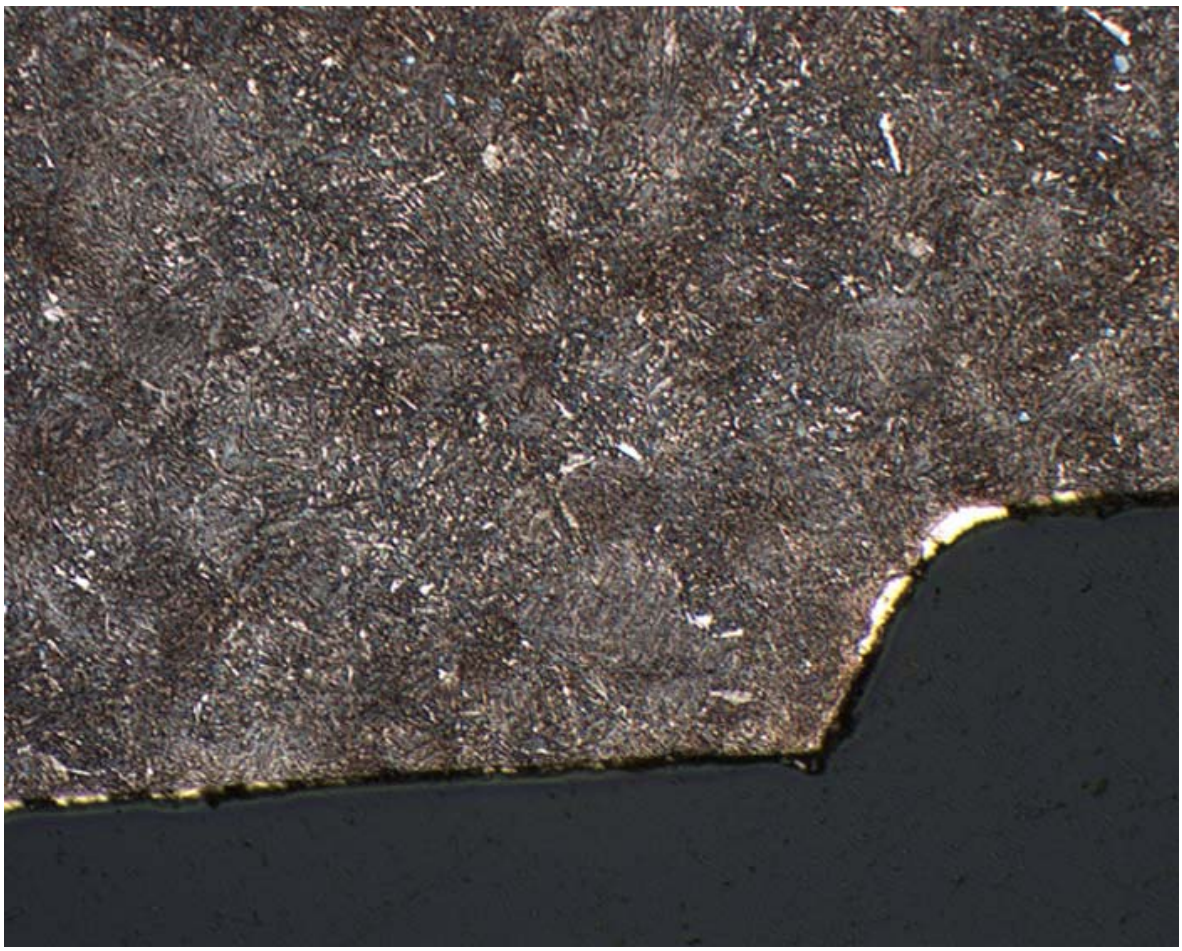

*Figure 3.2: Typical picture of the lands before shooting 25 shots (light microscopy.)*

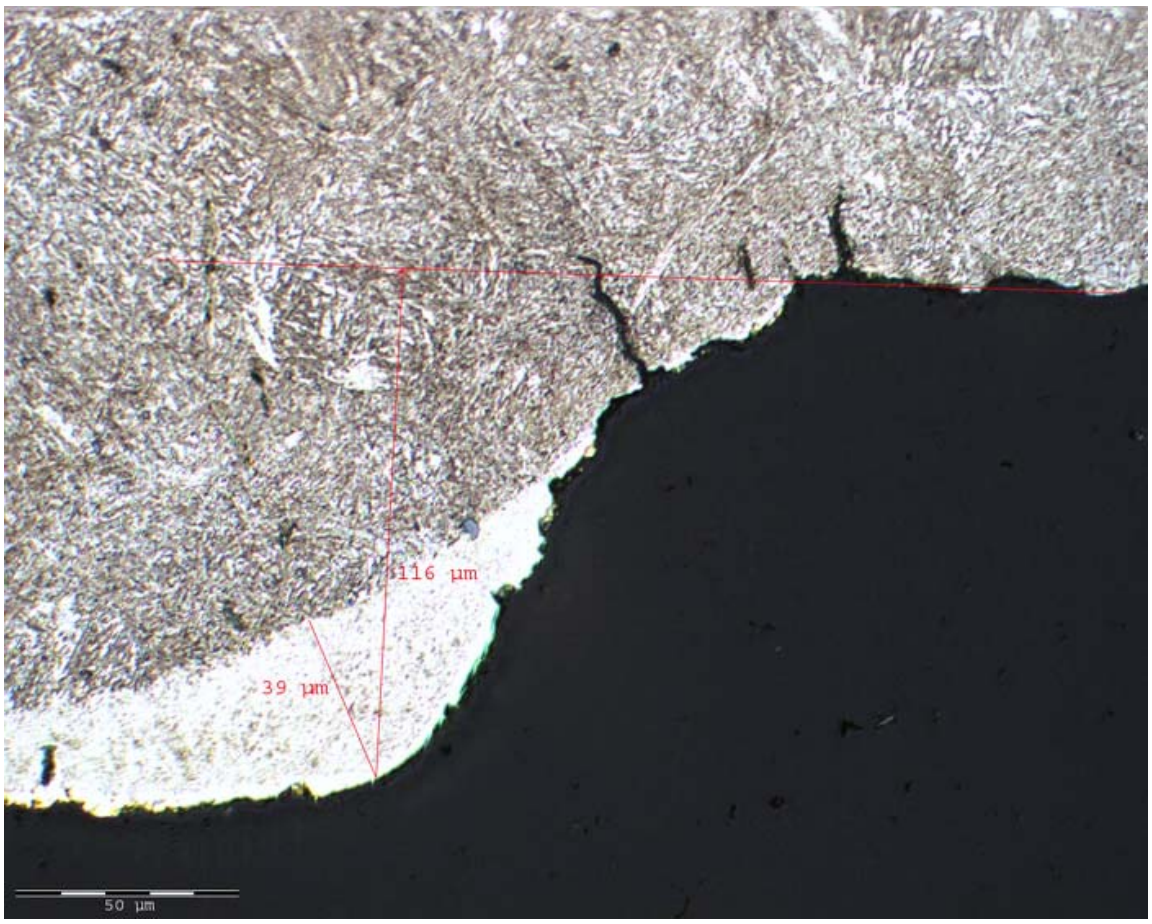


*Figure 3.3: The right side of the land after shooting 25 shots.*

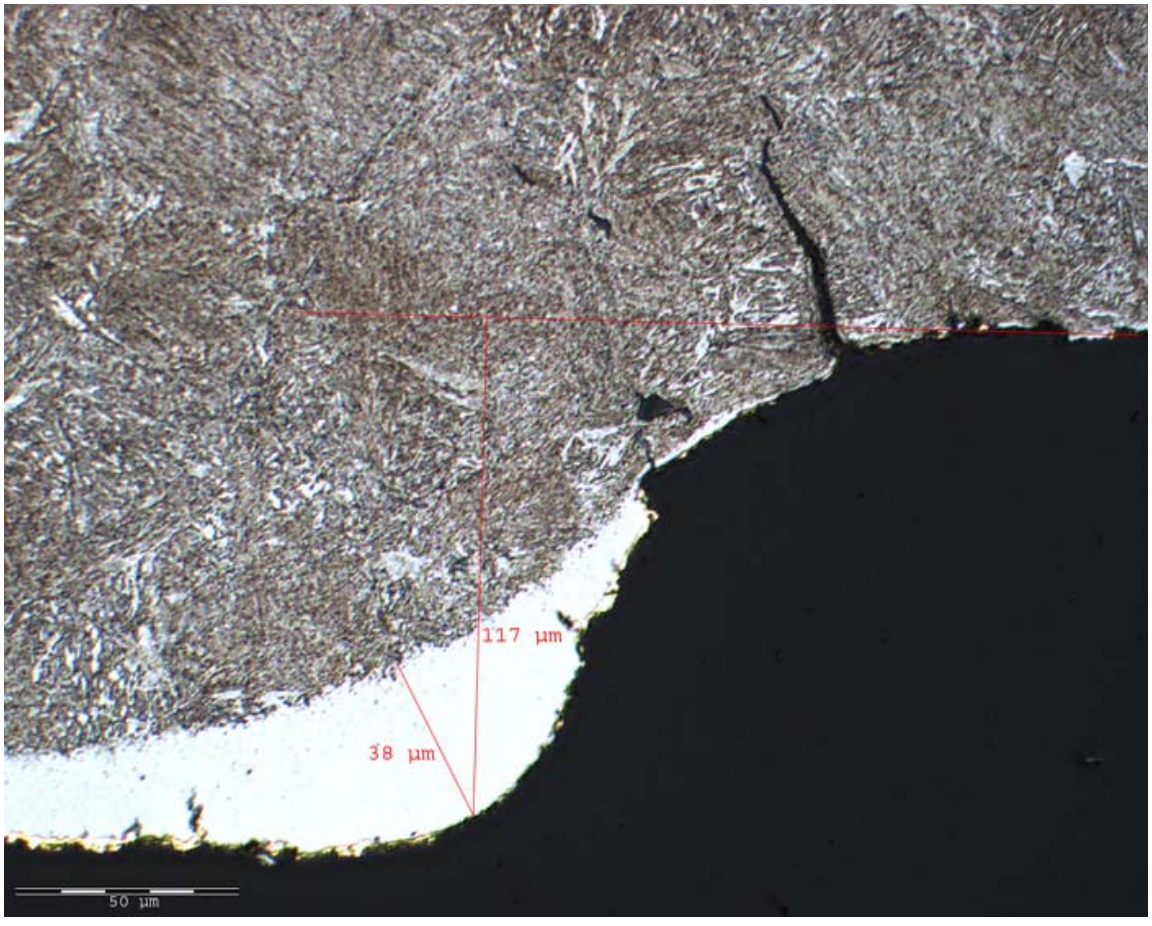


*Figure 3.4: The right side of the land after shooting 25 shots.*

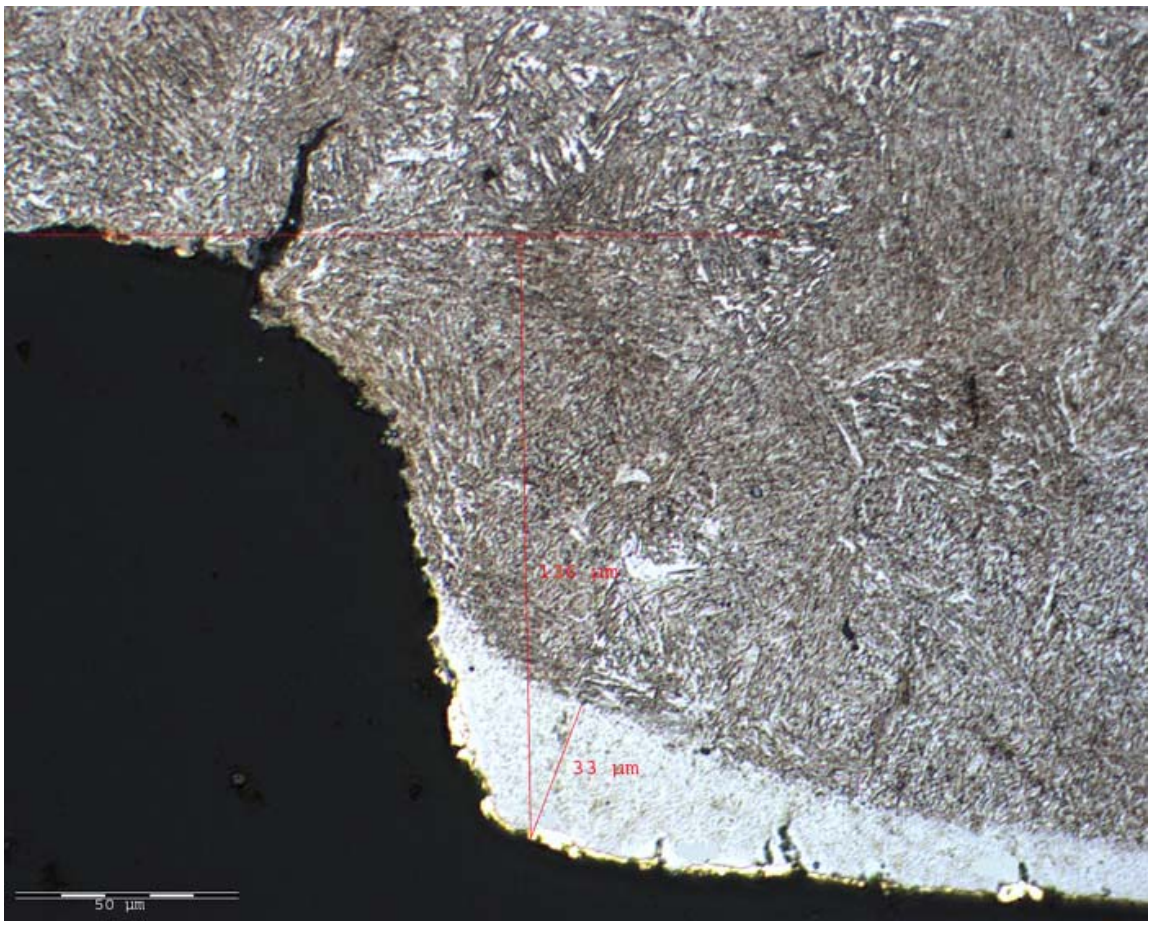


*Figure 3.5: The left side of the land after shooting 25 shots.*

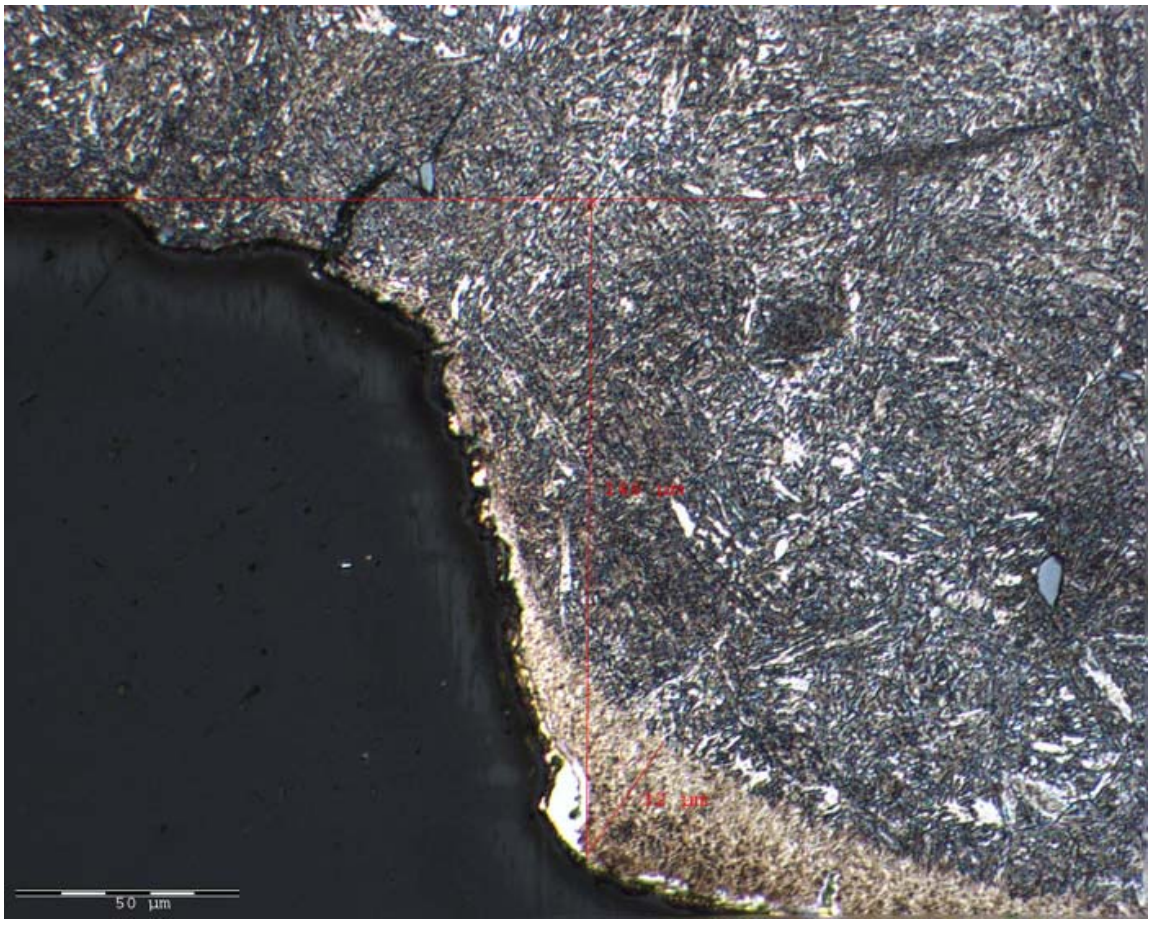


*Figure 3.6: The left side of the land after shooting 25 shots.*

| Heat affected region | | |
|---|---|---|
| Land no. | Left | Right |
| 1 | 33 | 39 |
| 2 | 32 | 38 |

| Thickness of lands | | |
|---|---|---|
| Land no. | Left | Right |
| 1 | 136 | 116 |
| 2 | 146 | 117 |

*Table 3.1: The geometric properties of the lands after 25 shots ( in micro meters)*

The Bofors NEXPLO was used, and the exit velocity of projectile was around 840m/s. The riffled length of the gun barrel was 77.2 cm (the riffled length of the complete gun barrel is 100.38 cm, giving an exit velocity of 920 m/s).

Three different zones are observed; a thin zone of approximately 1-5 micron consisting of Cu/Zn from the projectile. Thereafter a more directly heat affected zone of approximately 30-40 micron where a change in the structure of the steel has developed due to the high temperature and cooling rates during a shot. The metallurgic structure indicates that the region is a more frozen martensite structure developed due to temperature pikes around 1100 K. The original microstructure is an annealed martensite structure made during production of the gun barrel. We also observe that large cracks have developed in the neck of the grooves. We suggest that these cracks are developed due to large tensile forces produced by thermal stress near this region. We were not able to find the so called white layer of Iron Carbide (Fe3C and Iron Oxide (FeO). The reason for this is probably that we have shot too few shots.

To quantify the wear of the lands we defined two different measures. The first one is the maximum thickness of the heat-affected region measured normal to the land surface. After this distance is found, we measure the distance from the surface of the lands and the bottom part of the grooves (called the thickness of the lands). Figure 3.2-3.6 shows the two measured quantities. Table 3.1 show that the right side of the lands are more worn than the left side. This is believed to be due to the inertia forces from the projectile when it rotates with the twisting rifling.

A series of 25 shots was fired with projectiles that had been covered with varnish. The varnish cover is expected to reduce wear.


*Figure 3.7: The right side of the land after shooting 25 shots.* Varnish is used.

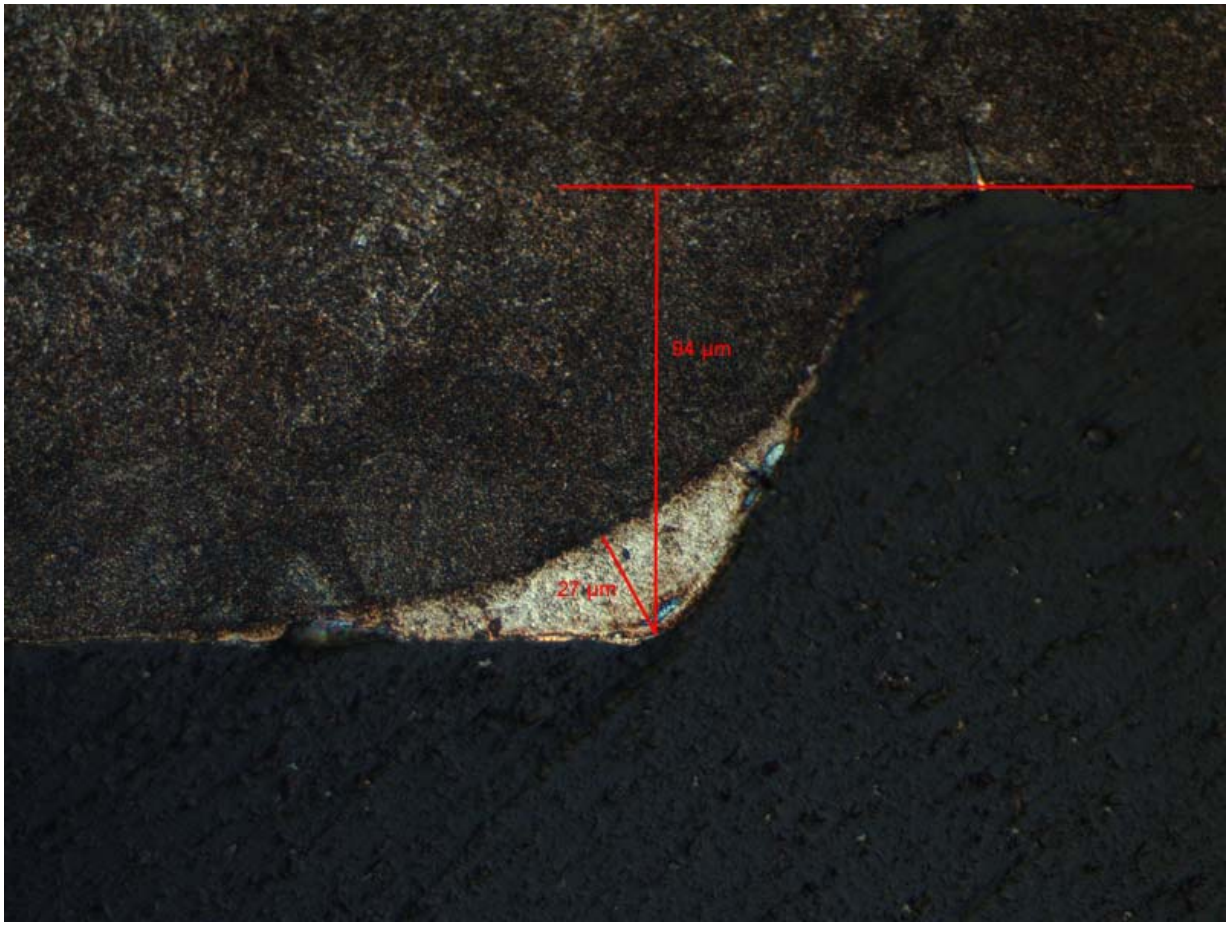


*Figure 3.8: The right side of the land after shooting 25 shots.* Varnish is used.

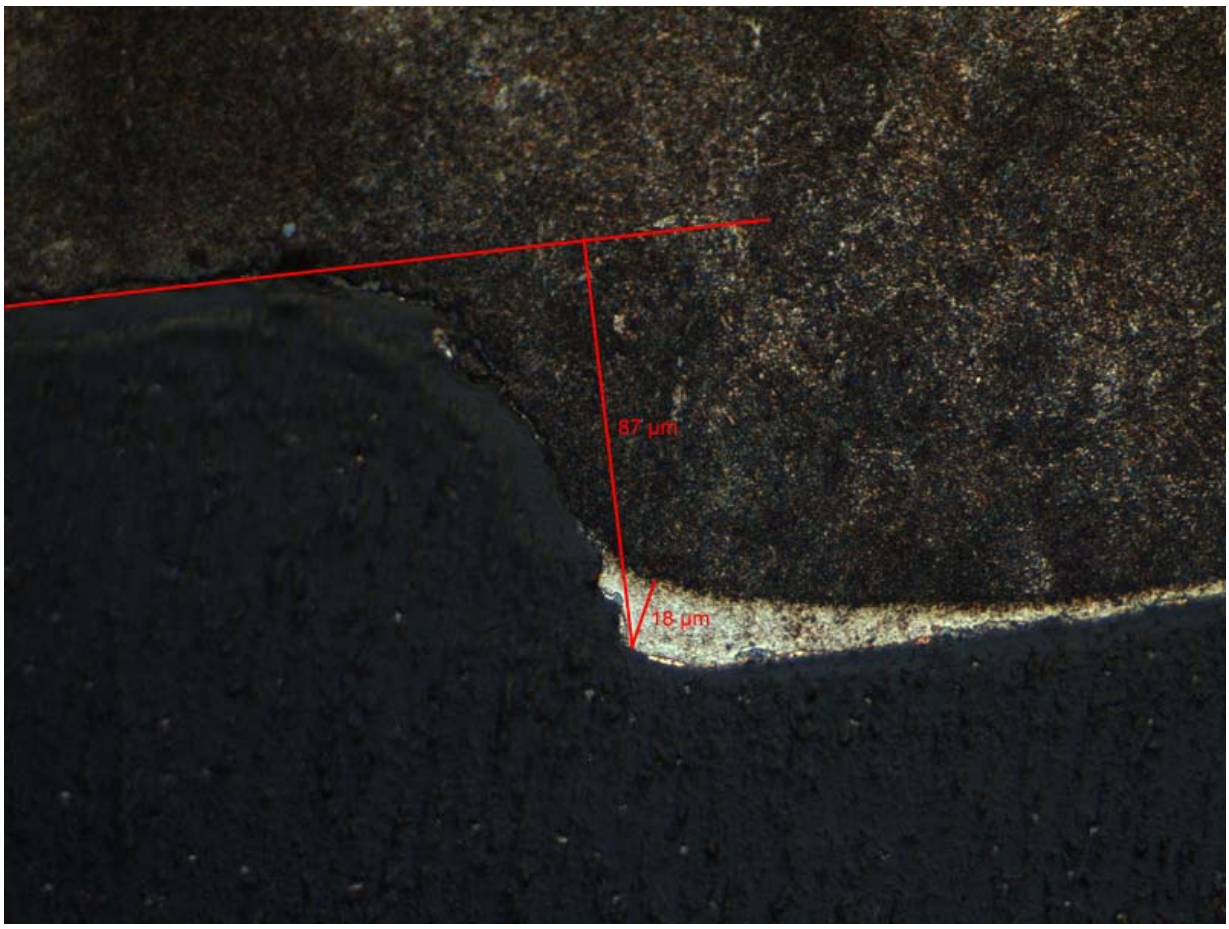


*Figure 3.9: The left side of the land after shooting 25 shots.* Varnish is used.

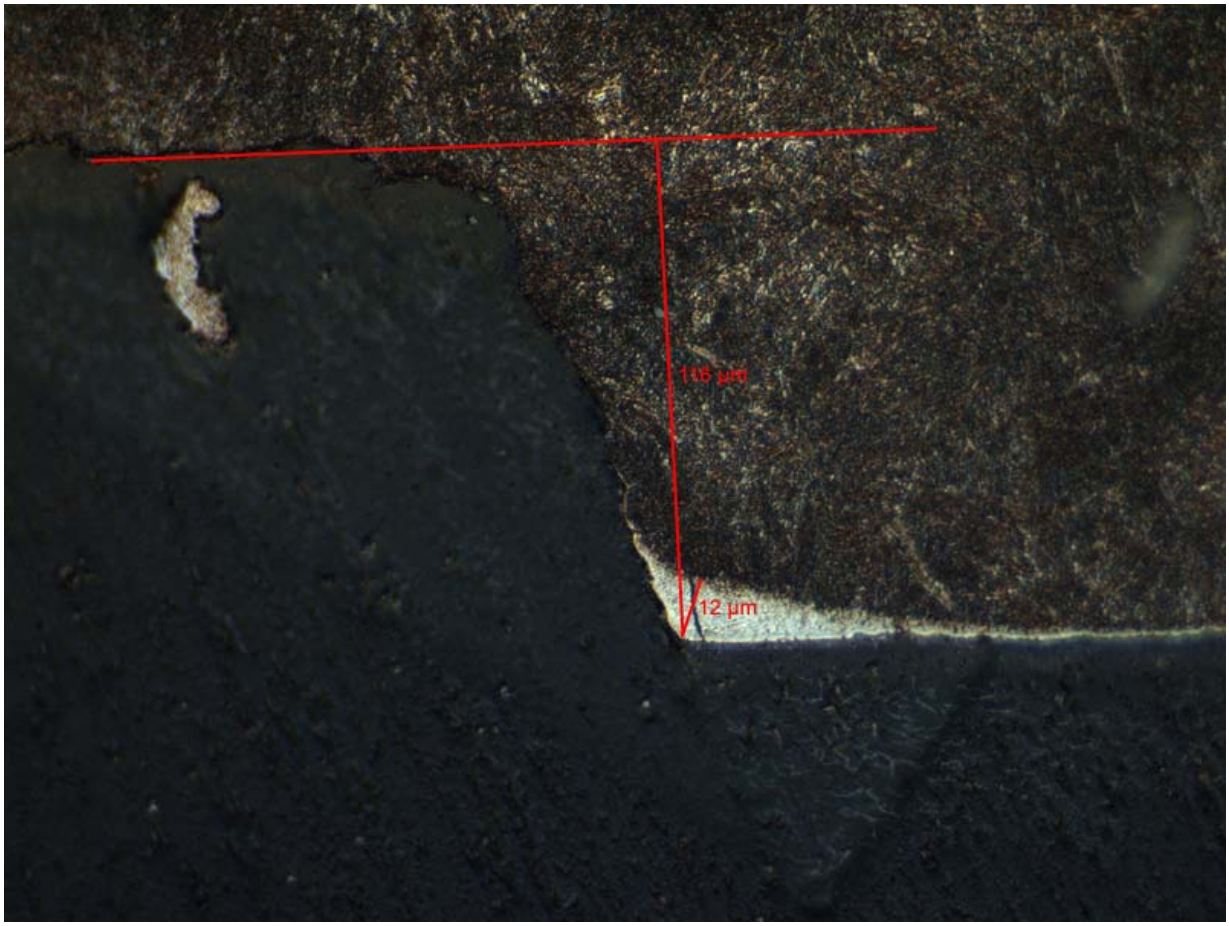


*Figure 3.10: The left side of the land after shooting 25 shots.* Varnish is used.

| Heat affected region | |
|---|---|
| Left | Right |
| 18 µm | 25 µm |
| 12 µm | 27 µm |

| Thickness of lands | |
|---|---|
| Left | Right |
| 87 µm | 84 µm |
| 116 µm | 94 µm |

*Table 3.2: The geometric properties of the lands after 25 shots (projectiles with varnish).*

Figures 3.7-3.10 show that the heat-affected region has been reduced when using the varnish. Thereby indicating less heating and less wear. Figure 3.11 is a simplified picture showing the heat-affected region on the lands in red and the unaffected material in blue. The asymmetric wear of the lands is clearly seen, as shown in tables 3.1 and 3.2.

Figure 3.12 and 3.13 shows how the heat-affected region looks like at the centre of the lands. It is difficult to say if there is a heat-affected region in figure 3.12 or just deposits of brass from the projectile. In figure 3.13 we observe more clearly both the heat-affected region and brass deposits from the projectile.

*Figure 3.11: Comparing lands from the shot series with varnish (lower) and without (upper).*

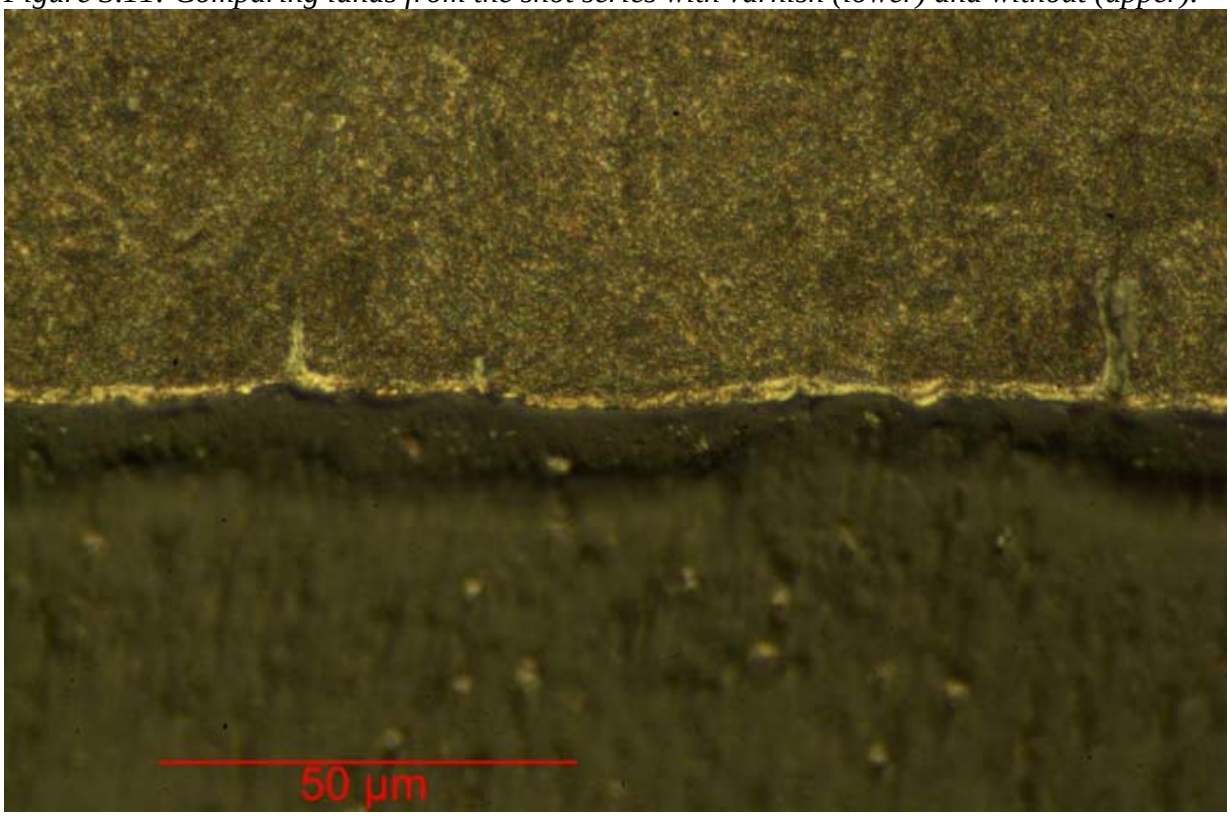


*Figure 3.12: Close-up of the centre of the land for shots with varnish.*

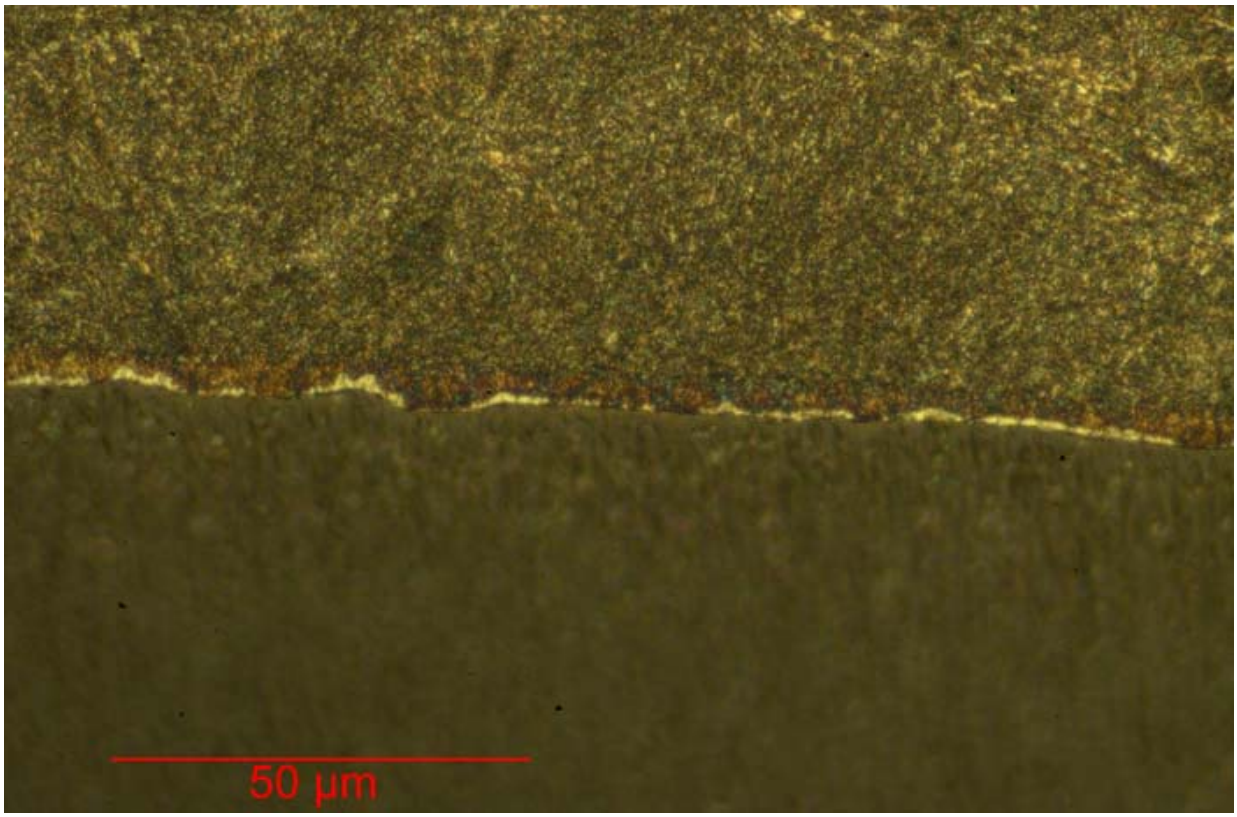


*Figure 3.13: Close-up of the centre of the land for shots without varnish.*

*Figure 3.14: Gun barrel used with varnish at projectile (left) and without varnish (right).*

To summarize the metallurgical and the light microscopy study: The in-frozen martensitic structure is clearly seen along the edges of the lands. Since carbon contend of the steel is originally 0.4 %, the phase diagram of steel shows the temperature should have been at least up to 1100K. The steel is originally annealed martensite, where the annealing temperature is around 700K. For some region of the gun barrel the temperature could have been above 700K

and below 1100K. For such regions the steel could have been softened. We have found that cracks develop significantly in the corner between the lands and the grooves. But also cracks are seen in the heat-affected region. Varnish reduces the thickness of the heat-affected region.

## 4 HARDNESS MEASUREMENTS

The hardness of the heat-affected region and the hardness of the original material in the gun barrel were measured. This was performed only for the gun barrel that fired the projectiles without varnish.

| | Diagonal [µm] | Force/Area [GPa] |
|---|---|---|
| 1 | 16,2 | 7,48 |
| 2 | 14,8 | 8,96 |
| 3 | 17,8 | 6,19 |
| Average | 16,3 | 7,54 |
| Std. Dev. | 1,5 | 1,38 |

*Table 4.1: The hardness based on Vickers diamond (pyramidal) indenter with 0.1 kg load in the heat-affected region after 25 shots. The hardness is defined as the force per unit of projected contact area.*

| | Diagonal [µm] | Force/Area [GPa] |
|---|---|---|
| 1 | 243 | 3,32 |
| 2 | 247 | 3,22 |
| 3 | 251 | 3,11 |
| Average | 247 | 3,22 |
| Std. Dev. | 4 | 0,10 |

*Table 4.2: The hardness based on Vickers diamond (pyramidal) indenter with 10 kg load in the base material. The hardness is defined as the force per unit of projected contact area.*

The measurements show that the heat-affected region is approximately a factor of 2 harder than the original material.

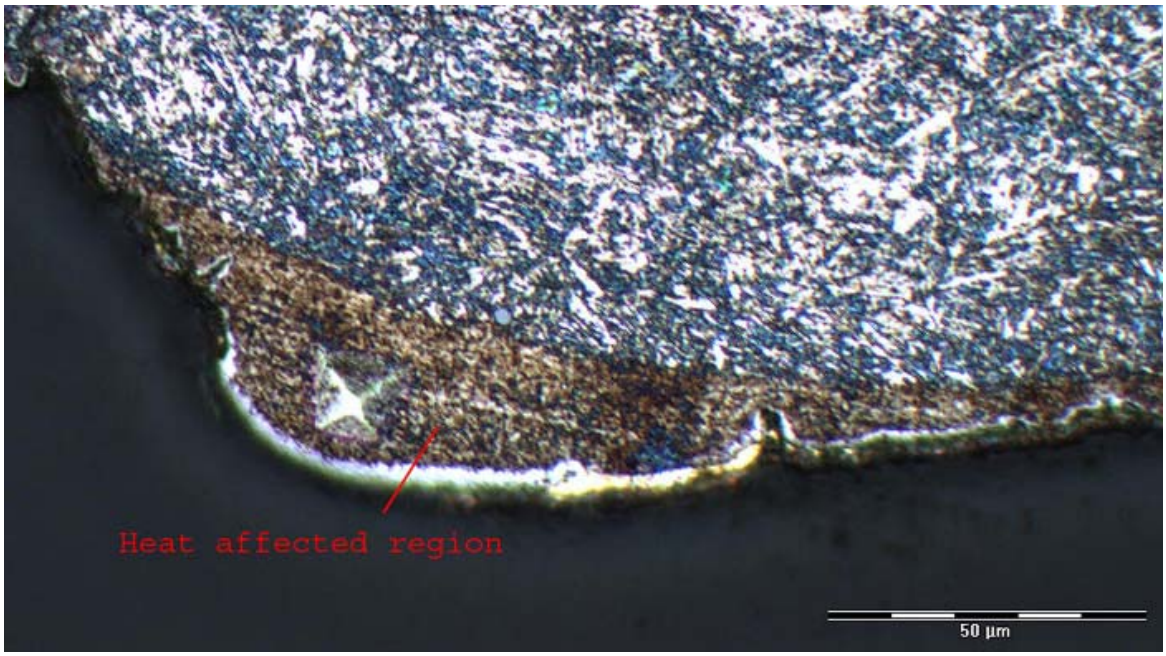

*Figure 4.1: Vickers indentation in the heat affected region.*

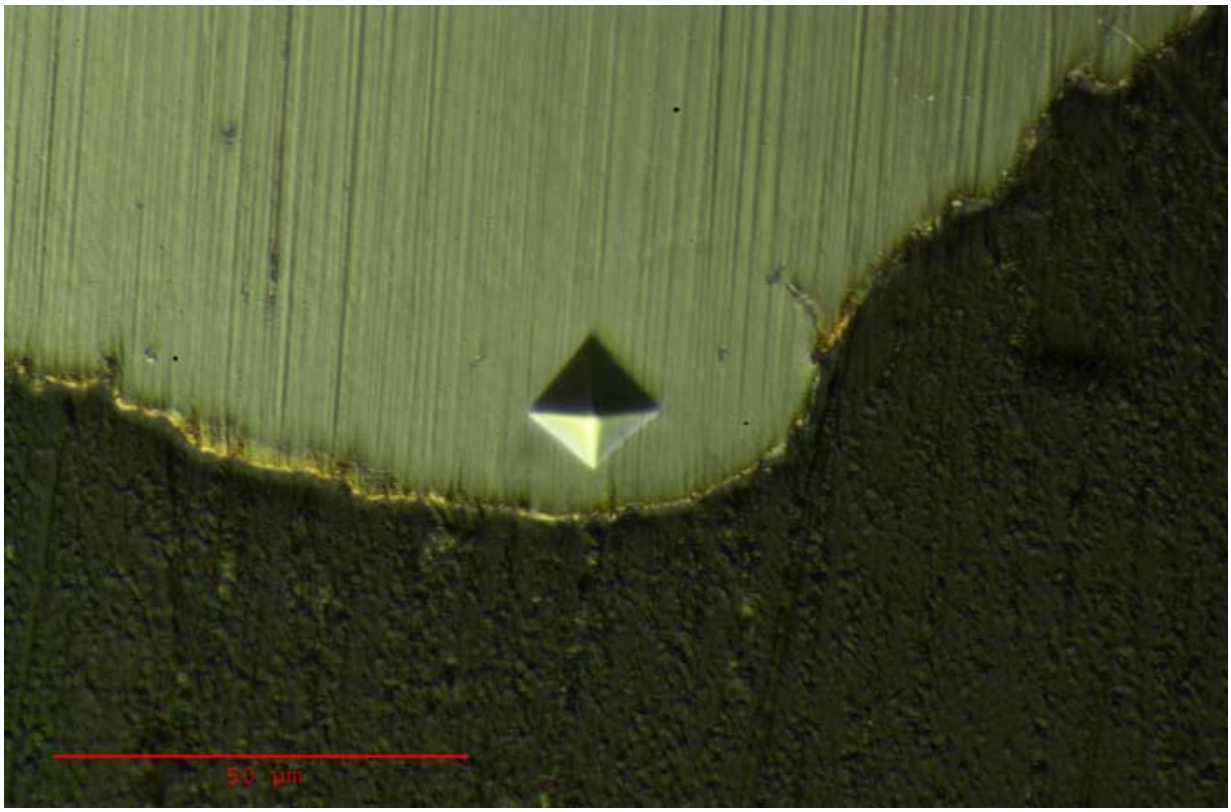


*Figure 4.2: Vickers indentation in the heat affected region.*

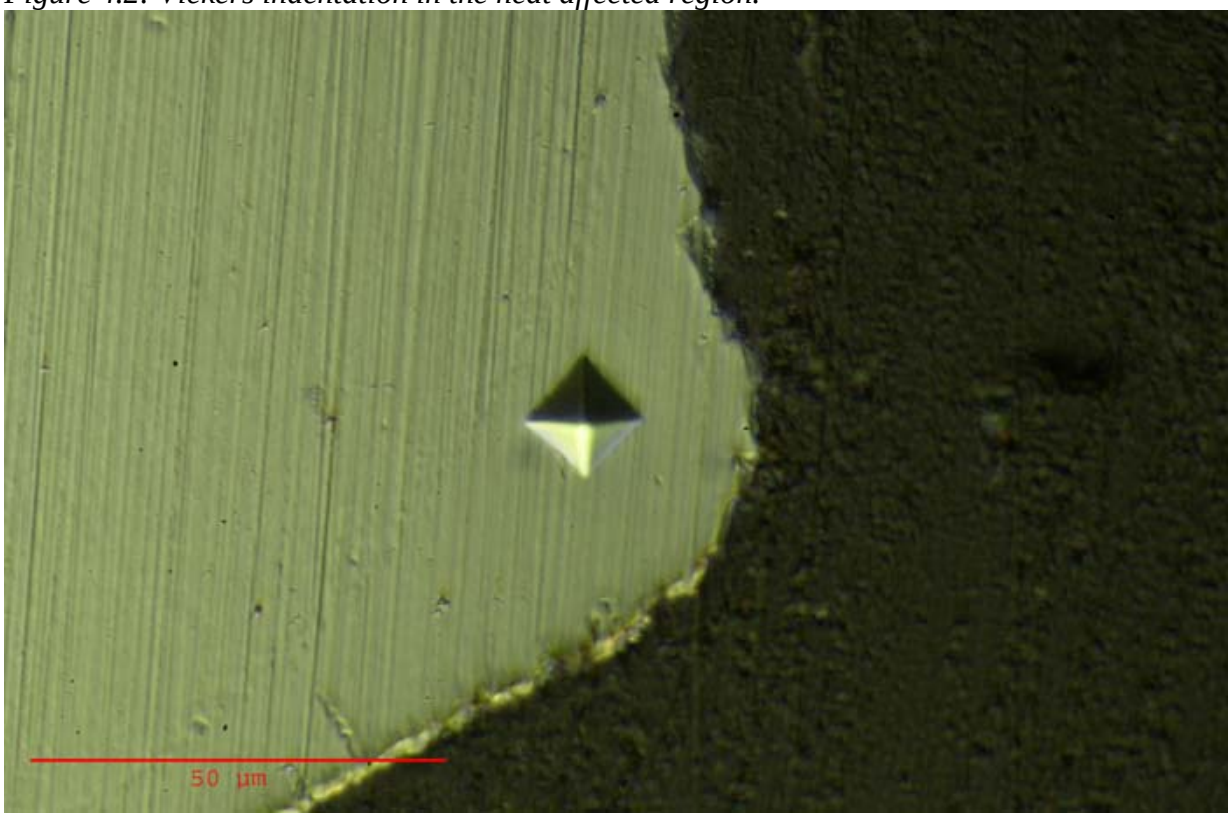


*Figure 4.3: Vickers indentation in the heat affected region.*

To summarize the hardness measurements; the heat-affected region was approximately a factor of two harder than the original steel structure. This is in agreement with the proposed martensitic structure in this region. (Picture of the structure)

## 5 SCANNING ELECTRON MICROSCOPY

To analyse the gun barrel steel more intensively we also performed the Scanning electron microscopy together with an EDS analysis.

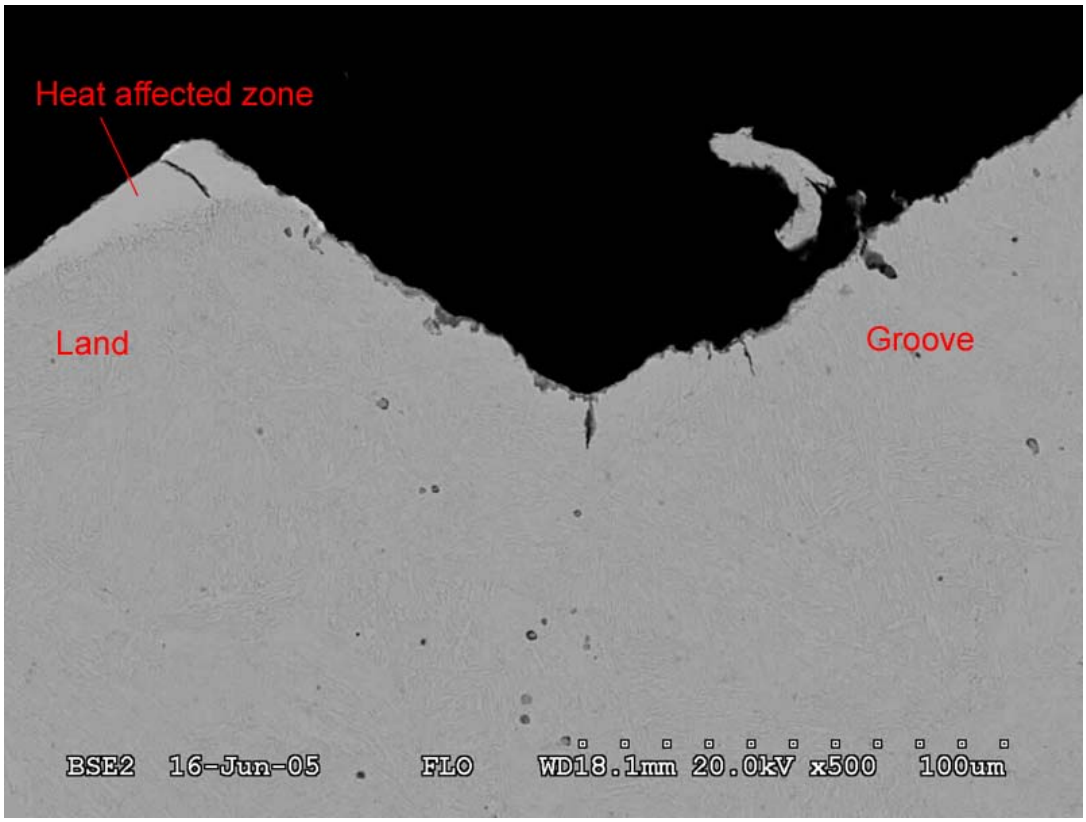


*Figure 5.1: Backscatter image showing cracks in both heat affected zone on the land and tempered martensite in the groove.*

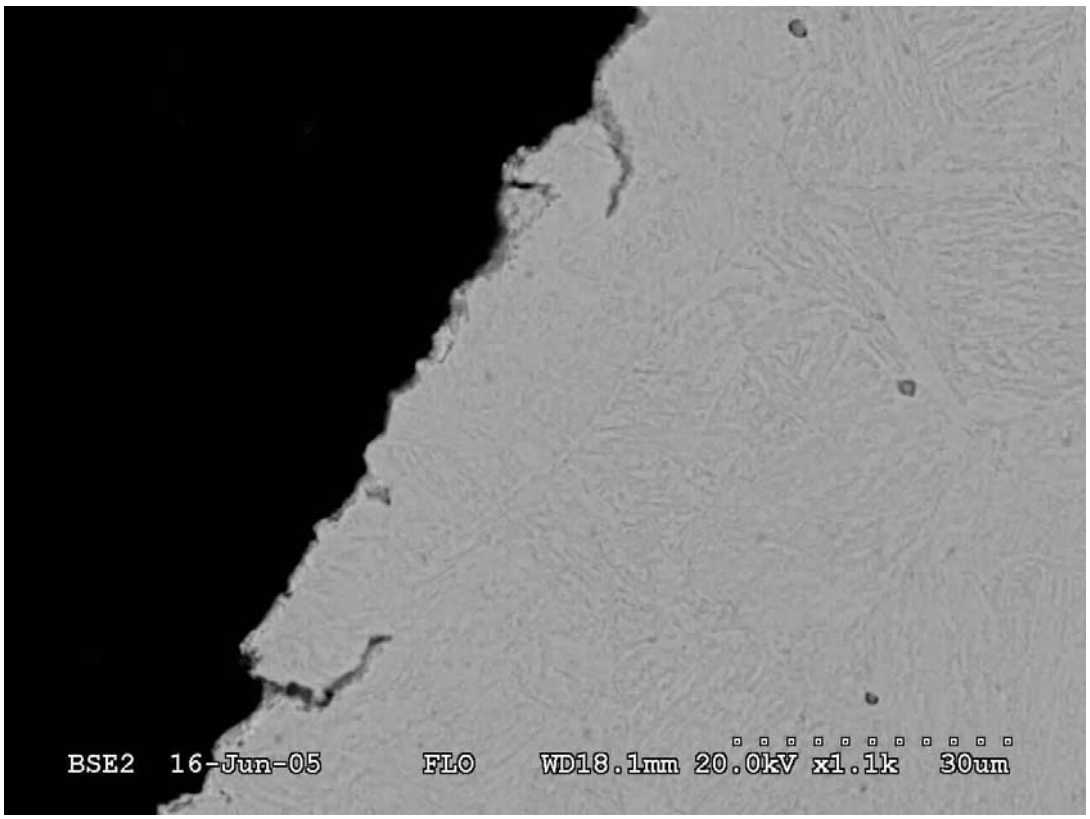


*Figure 5.2: Backscatter image showing cracks in the tempered martensite in the groove.*

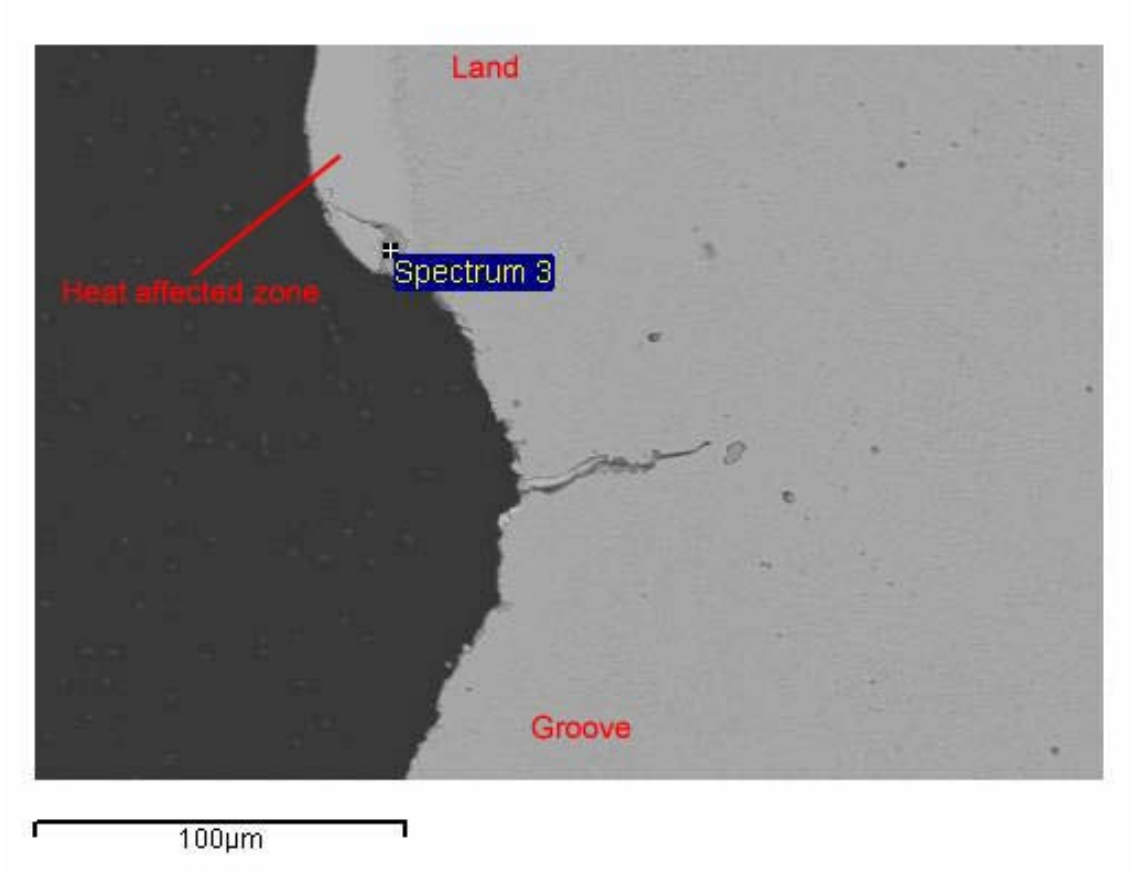


*Figure 5.3: Backscatter image of the EDS analysis spot in a crack in the heat affected zone.*

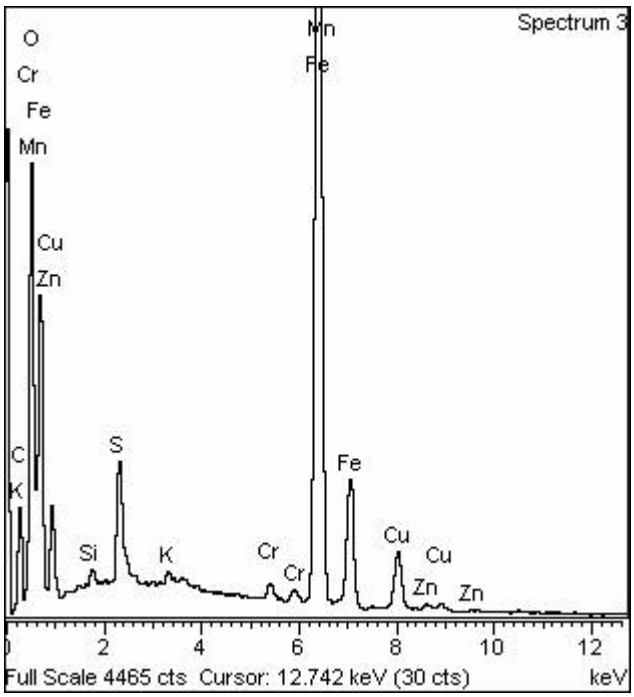


*Figure 5.4: EDS analysis of spectrum 3 in figure 5.3.*

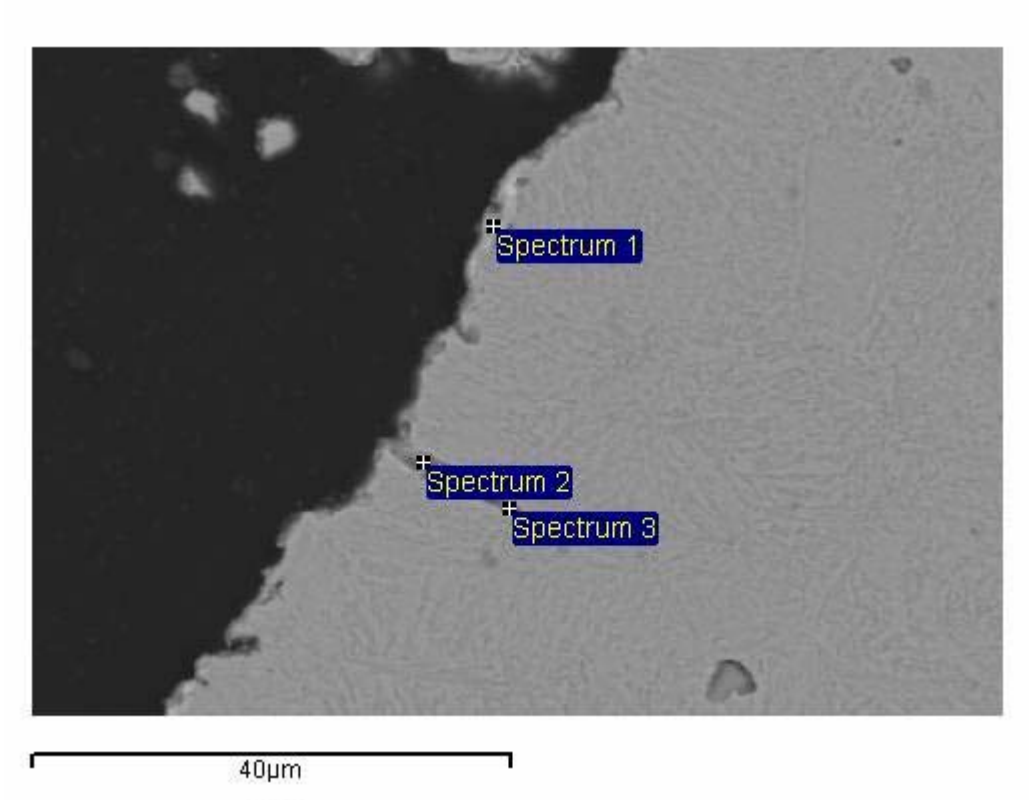


*Figure 5.5: Backscatter image of the EDS analysis spots.*

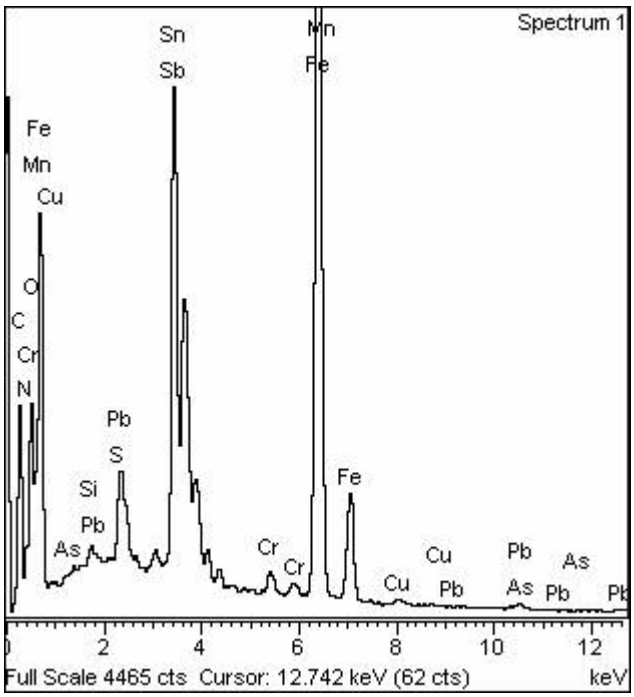


*Figure 5.6: EDS analysis of spectrum 1 in figure 5.5.*

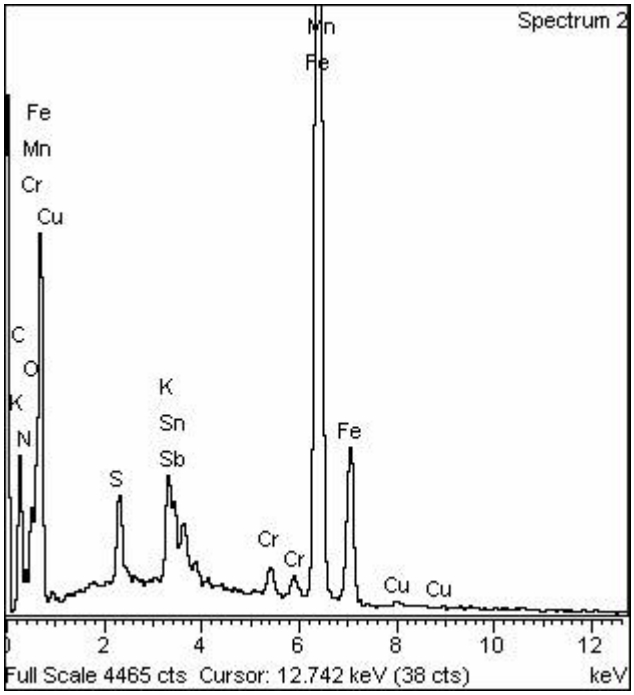


*Figure 5.7: EDS analysis of spectrum 2 in figure 5.5.*

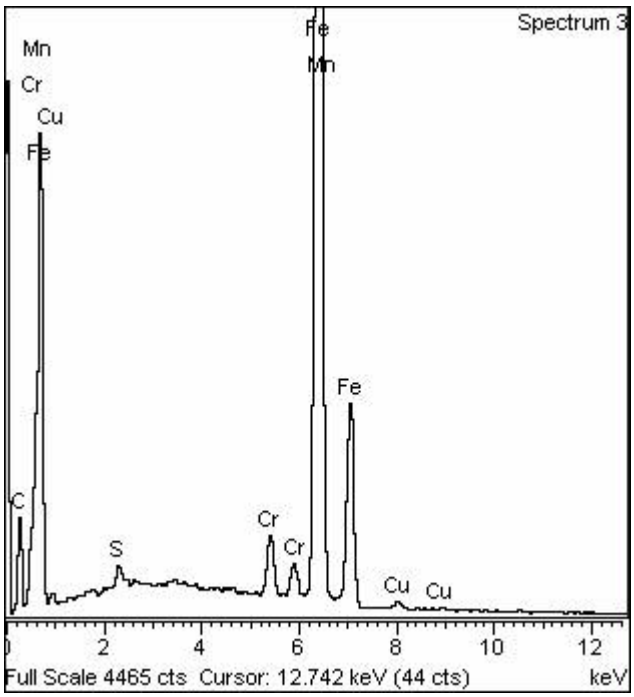

Figure 5.8: EDS analysis of spectrum 3 in figure 5.5.

Figures 5.1-5.8 show typical SEM pictures. We find large cracks both in the heat-affected regions on the lands and in the tempered region in the grooves. The EDS analyses show that residues of the gun barrel gases were deposited in the cracks.

## 6 ELECTRON PROBE MICRO ANALYSER (EPMA)

By using EPMA measurements the atomic content of the gun barrel was measured from the surface of the lands and inward with a step length of 2 microns. Of special interest was to study the carbon content since the amount of Carbon is not sufficiently revealed by using the EDS analysis. The actual values of the carbon content is not trust worth but relative values should be correct. It was found that the chemical content of the heat-affected region was the same as for the unused gun barrel.

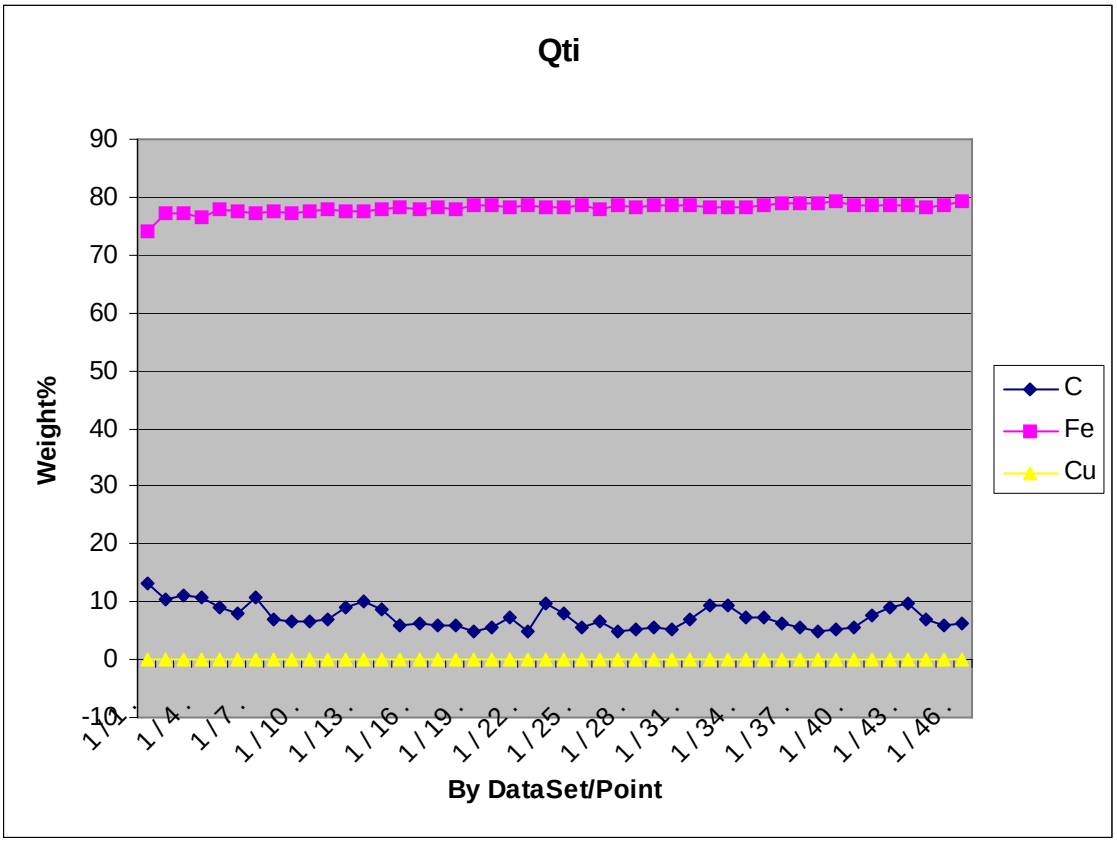


*Figure 6.1: EPMA measurements run no. 1 (appendix A for numerical values).*

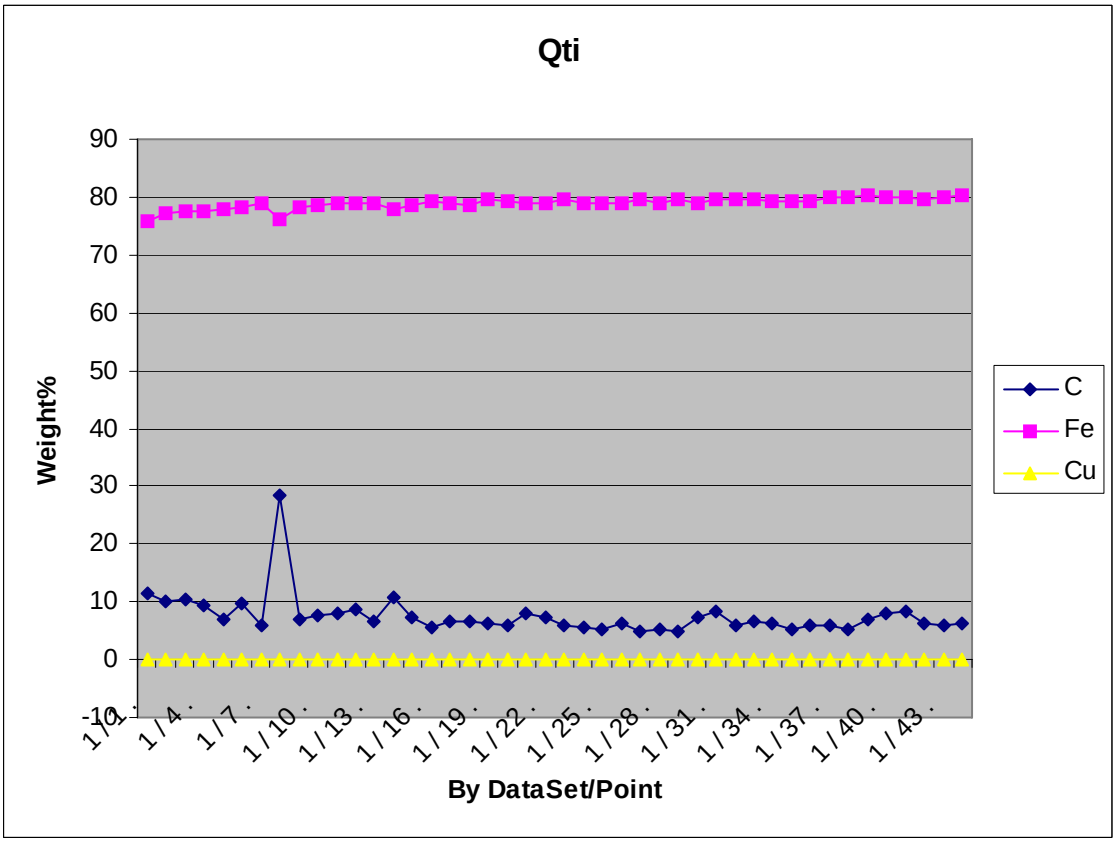


*Figure 6.2: EPMA measurements run no. 2 (appendix A for numerical values).*

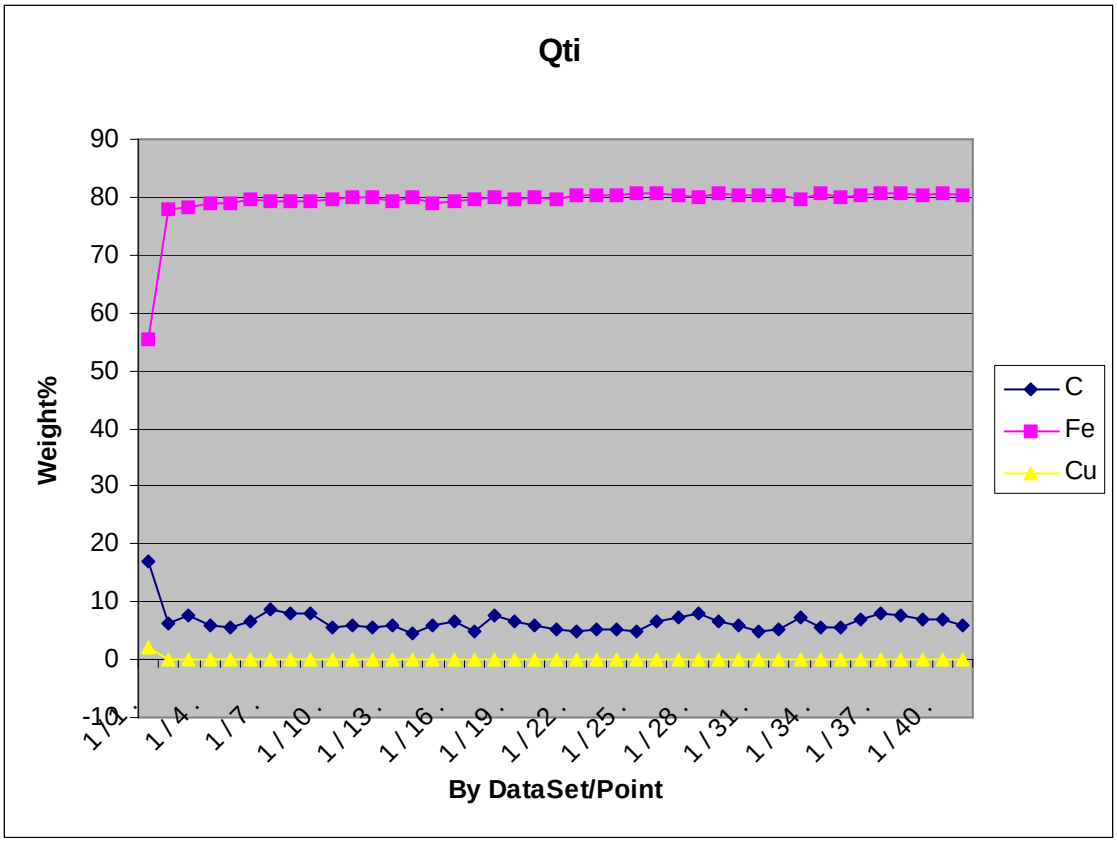


*Figure 6.3: EPMA measurements run no. 3 (appendix A for numerical values).*

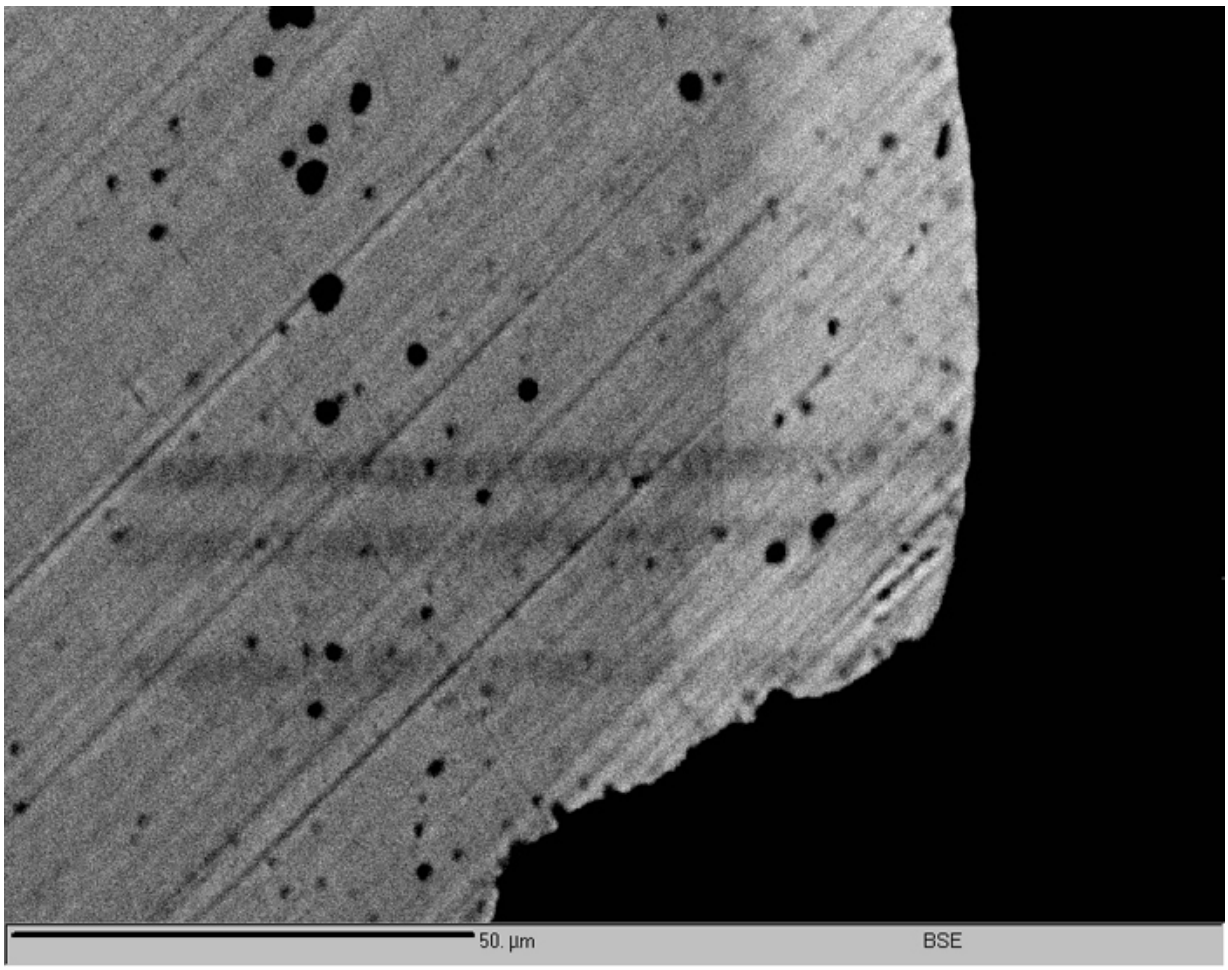


*Figure 6.4: Backscatter image of the three EPMA runs. Run 3 are the lowest one.*

The carbon content did not change when passing into the heat-affected region (approximately 10-15 points from the surface in figures 6.1-6.3). Figures 6.1 and 6.2 could indicate a small carbon enhancement close to the gun barrel surface, but since the sample is encapsulated in epoxy mounting, this result is unreliable.

Figures 6.5-6.8 shows two EPMA runs taken on a discarded gun barrel that is heavily worn. The content of copper increases close to the surface. Also, the carbon content increases but since the sample is encapsulated in an epoxy mounting this result is somewhat unreliable.

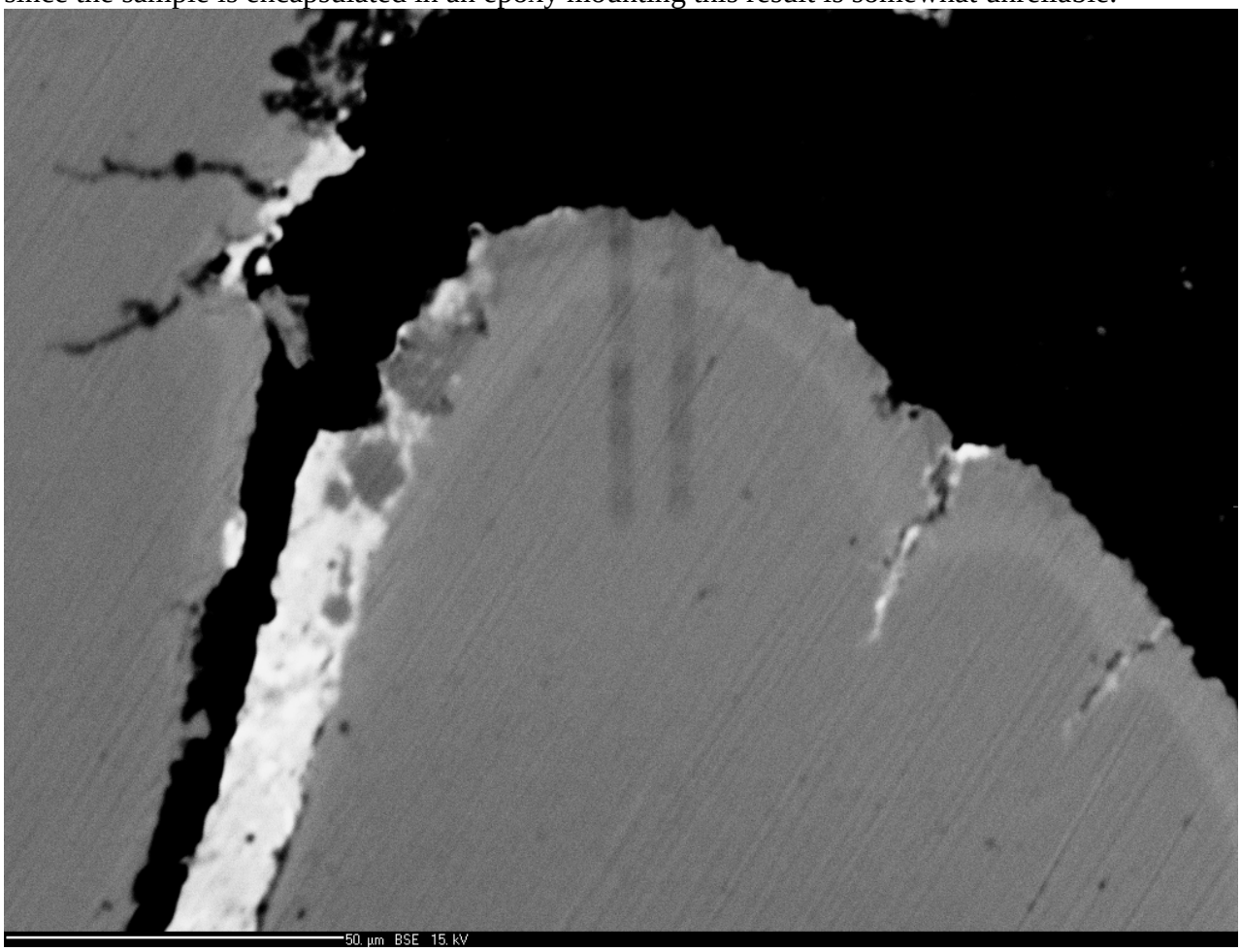


*Figure 6.5: EPMA runs on discarded gun barrel. Run 1 on the left. 2 microns step length from the inner region and outwards.*

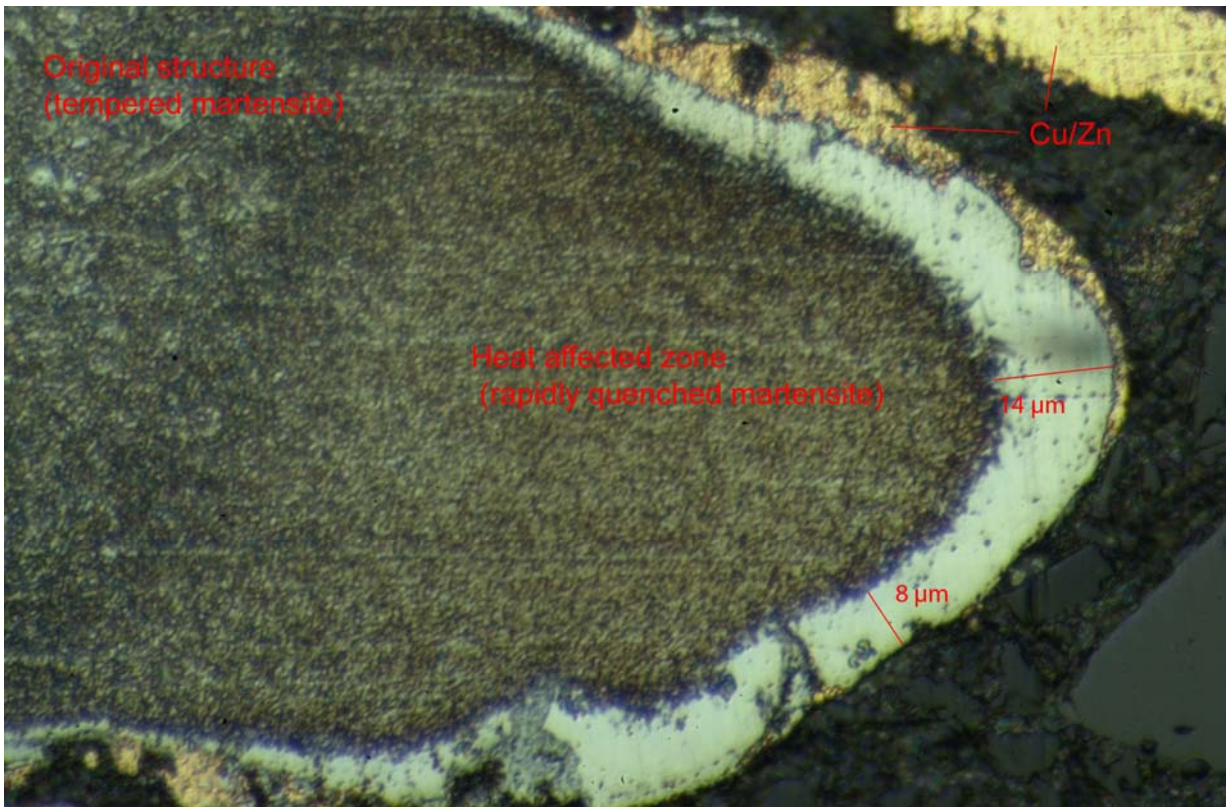


*Figure 6.6: Picture taken in optical microscope of the same area as in figure 5.5. Denotes the different regions.*

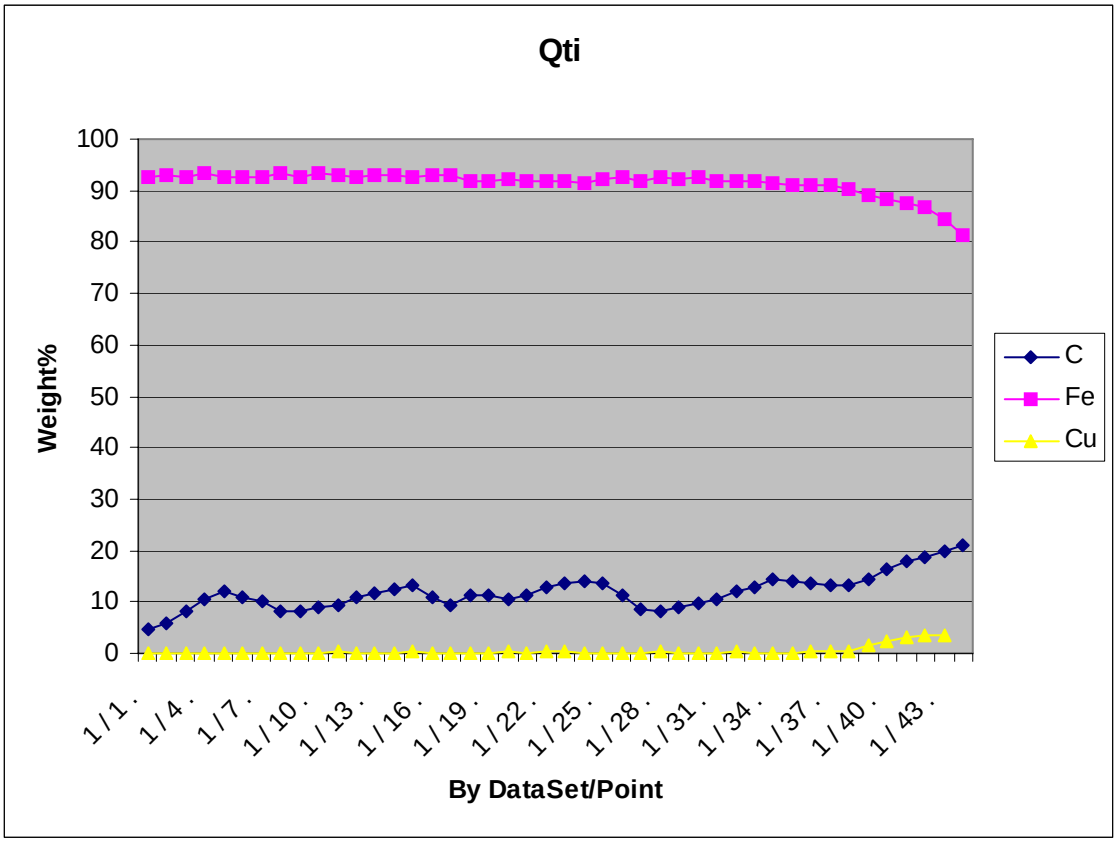


*Figure 6.7: EPMA run no. 1 on discarded gun barrel.*

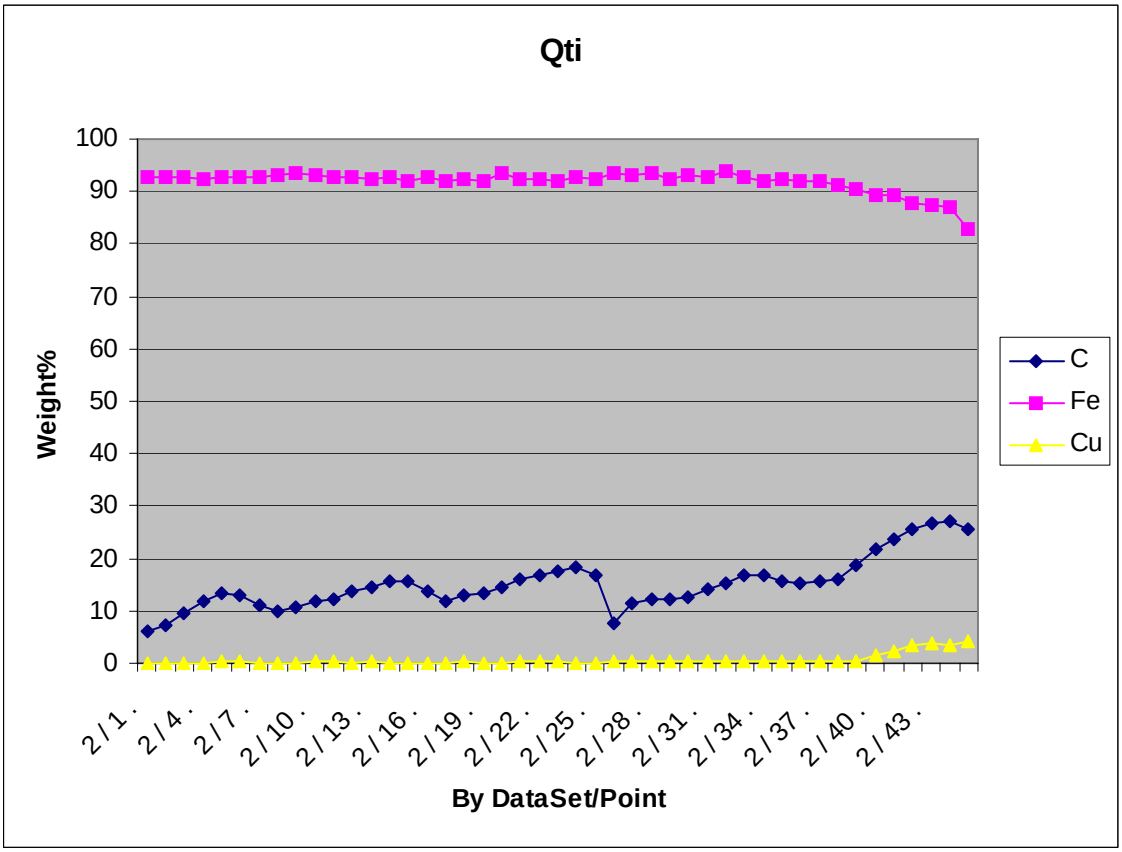


*Figure 6.8: EPMA run no. 2 on discarded gun barrel.*

There is a somewhat higher concentration of carbon in the white layer. We believe that this result is trustworthy. Probably the white layer consists of cementite. The experimental result is in close agreement with the results of [16]-[17].

The general conclusion is that the heat-affected zone is unaffected by chemical species from the gun barrel gases. The increased hardness is due to morphological changes in steel structure caused by large temperatures up to 1100K and large heating and cooling rates. The morphological structure is believed to be a "frozen" martensitic structure. The outer white layer of 14 microns in figure 5.6 is believed to be a chemically affected zone. It is probably mainly cementite.

## 7 THEORETICAL CALCULATIONS OF THE FRICTION FORCE

In this section we analyse more theoretically the necessary friction force to give the heat-affected region. We assume

$$\underbrace{\underbrace{f_f}_{\text{Friction force}}\ \underbrace{u}_{\text{Velocity}}\ \underbrace{\Delta t}_{\text{Time interval}}}_{\text{Friction energy}} \overset{mod}{=} \underbrace{\rho}_{\text{Density}}\ \underbrace{c_v}_{\text{Heat capacity}}\ \underbrace{a}_{\text{Width of lands}}\ \underbrace{h}_{\text{Tickness of heat-affected region}}\ \underbrace{\Delta T}_{\text{Temperture increase}}\ \underbrace{8}_{\text{Number of lands}} \qquad (7.1)$$

Using that $\Delta t = L/u$, where L is the maximum length of the contact surface between the projectile and the gun barrel surface, gives that

$$f_f = \frac{8\rho c_v a h \Delta T}{L} \tag{7.2}$$

Inserting that

$$\rho = 7800 \text{ kg/m}^3,\ c_v = 450 \text{ J/(kgK)},\ a = 1.7\,10^{-3} \text{ m},\ L = 1.5\,10^{-2} \text{ m}$$
$$h = 10^{-5} \text{ m (Experimental)},\ \Delta T = 700 \text{ K(Experimental)} \tag{7.3}$$

gives that

$$f_f = \frac{8\ 7800\ 450\ 1.7\,10^{-3}\ 10^{-5}\ 700}{1.5\,10^{-2}} \approx 2.2\,10^4 \text{ N} \tag{7.4}$$

This value is in good agreement with the measured quasi static in pressing force of projectiles reported in the next section.

Instead of using the measured values of the depth of the heat affected region we can use that

$$\underbrace{h}_{\substack{\text{Tickness of}\\ \text{heat-affected region}}} = \left( \frac{\underbrace{\kappa}_{\text{Conductivity}}}{\rho c_v} \Delta t \right)^{1/2} = \left( \kappa L / \left( \rho c_v u \right) \right)^{1/2} \tag{7.5}$$

Using that

$$\kappa = 20 \text{ W/(mK)},\ u \approx 100 \text{ m/s}\left(\text{assumed}\right) \tag{7.6}$$

finally gives that

$$h = \left( \frac{20}{7600\ 450} \frac{0.015}{100} \right)^{1/2} \approx 3\,10^{-5} \text{ m} \tag{7.7}$$

This is in good agreement with the experimental results in equation (7.3).

The movement of the projectile into the gun barrel can conceptually be considered as a situation where the hard lands penetrate into the projectile copper jacket. The force necessary to penetrate the 8 lands should then according to familiar indentation theory be given by

$$\underbrace{f_p}_{\text{Indentation force}} = \underbrace{8}_{\text{Number of lands}}\ \underbrace{H}_{\text{Hardness}}\ \underbrace{a}_{\text{Width of land}}\ \underbrace{b}_{\text{Height of land}} \tag{7.8}$$

where b is the height of the lands and H is now the hardness of the projectile jacket. Using that

$$a = 1.7\,10^{-3} \text{ m},\ b = 1.5\,10^{-5},\ H = 1.3\,10^9 \text{ Pa(measured)} \tag{7.9}$$

gives that

$$f_p = 8Ha\,b = 8\,1.3\,10^{9}\,1.7\,10^{-3}\,1.5\,10^{-4} = 2.6\,10^{3}\ \text{N} \tag{7.10}$$

This force is one order of magnitude smaller than the frictional force.

## 8 THE PENETRATION FORCE OF THE PROJECTILE INTO THE GUN BARREL

The frictional force calculated in section six has been supported by measurements using a special designed tool. Figure 8.1 shows the tool.

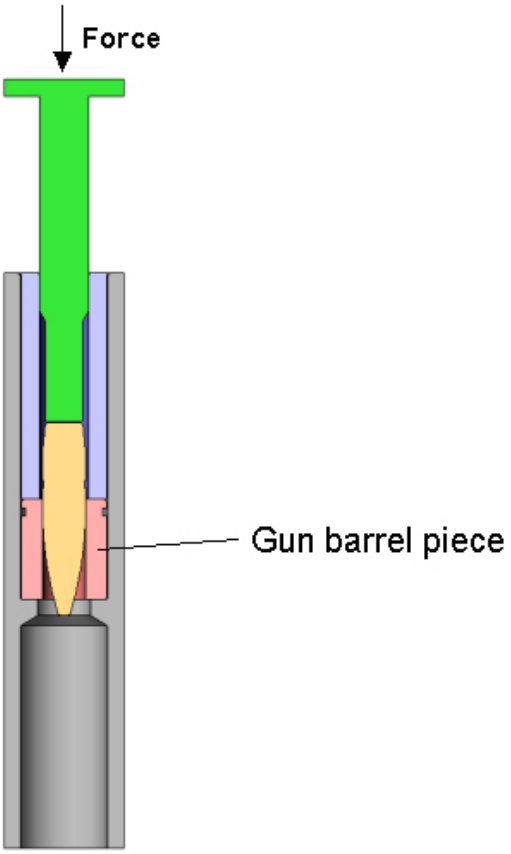


*Figure 8.1: A specially designed tool used for force measurements.*

Theoretically is the force as a function of penetration distance, according to our design, approximately given by

$$\underbrace{f(x)}_{\substack{\text{Force to press the}\\ \text{projectile into the}\\ \text{gun barrel}}} = \begin{cases} \underbrace{f_p}_{\text{Indentation force}} + 8 \quad \underbrace{\mu}_{\text{coefficinet of friction}} \quad \underbrace{\sigma}_{\text{Normal stress}} \quad \underbrace{a}_{\text{Width of lands}} \quad \underbrace{x}_{\text{Penetration depth}} & \text{when } x \le 1.8 \text{ cm} \\ f_p + 8\mu\sigma a\,1.8 \;\; when \; 1.8cm \le x \le 2.8cm & \\ f_p + 8\mu\sigma a\,1.8 + 8\mu\sigma a\,(2.8 - x) \;\; when \; 2.8 \le x \le 2.8cm + 1.8cm & \end{cases} \tag{8.1}$$

where $\mu$ is the friction coefficient, x is the penetration distance and $\sigma$ is the normal force on the surface of the lands.

The maximum normal stress on the lands are from (8.1) approximately given as

$$\sigma \approx \frac{f}{8\mu a x} \tag{8.2}$$

Inserting that

$$f \approx 3\,10^4 \text{ N (Experimentally)}, \mu \approx 0.1 \text{ (Guessed)}, x \approx 0.018 \text{ m} \tag{8.3}$$

finally gives

$$\sigma = \frac{f}{8\mu a x} = \frac{3\,10^4}{8\;0.1\;0.0017\;0.018} = 1.2\,10^9 \text{ Pa} \tag{8.4}$$

This value is in good agreement with the hardness of the projectile (as it should be).

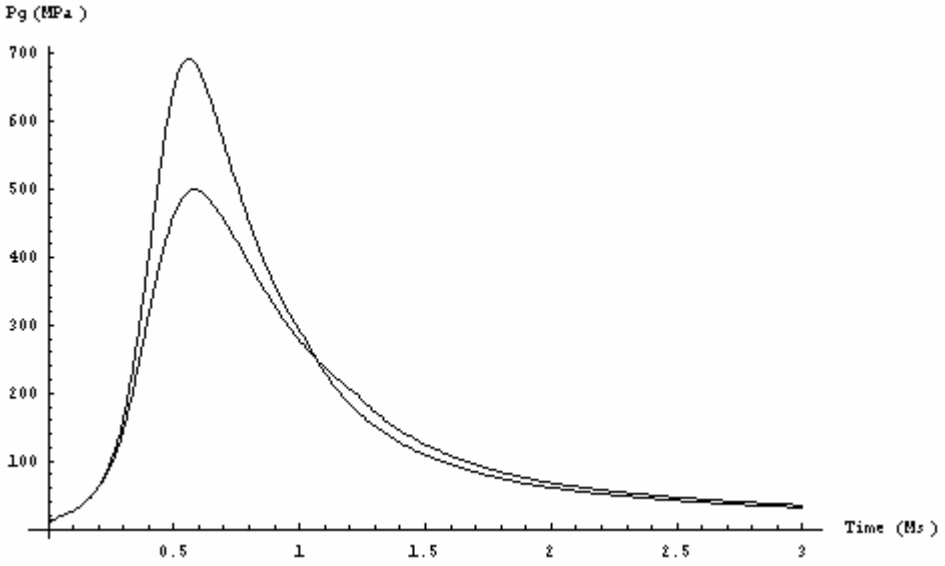


*Figure 8.2: The pressure in the gun barrel using two different forces between the gun barrel and the projectile. Upper curve is based on the total force. Lower curve is based on the indentation force only.*

The relative area of the load bearing area of the recoil system and the projectile base is given by

$$\underbrace{\bar{A}}_{\text{Relative area}} = \frac{\pi\left(\underbrace{\bar{C}}_{\text{Calibre of cartridge}}/2\right)^2}{\underbrace{D}_{\text{With of grip zone}}\;\underbrace{d}_{\text{Hight of grip zone}}} \tag{8.5}$$

Using that

$$\bar{C} = 0.02 \text{ m}, \; D = 0.02 \text{ m}, \; d = 3\cdot 10^{-3} \text{ m} \tag{8.6}$$

gives

$$\bar{A} = \frac{\pi\left(\bar{C}/2\right)^2}{Dd} = \frac{\pi\left(0.02/2\right)^2}{0.02\,0.003} \approx 5 \tag{8.7}$$

The yield stress of the recoil bolt is approximately 2 GPa. The critical pressure in the cartridge necessary to achieve yield in the recoil bolt is then

$$p_c = \lambda\ 2\ \text{GPa} / \bar{A} \approx 400\ \text{MPa},\ \lambda \approx 1 \tag{8.8}$$

This pressure is of the same magnitude as the pressure of the gun barrel gases. Thus indicating that strength of the recoil bolt is marginal.

## 8.1 Measurements of the force pressing the projectile into the gun barrel

Several types of projectiles were tested. Typical values of the penetration force are between 20 – 30 kN.

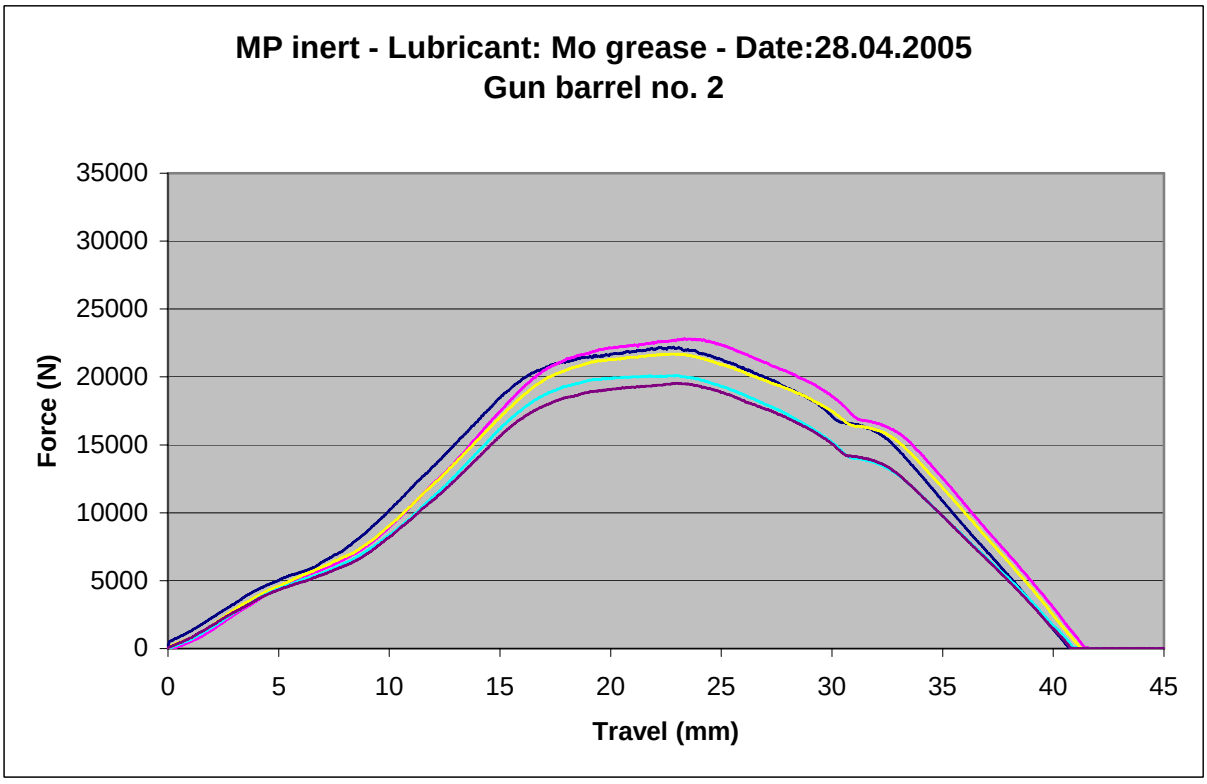


*Figure 8.1: The measured force as a function of the penetration distance.*

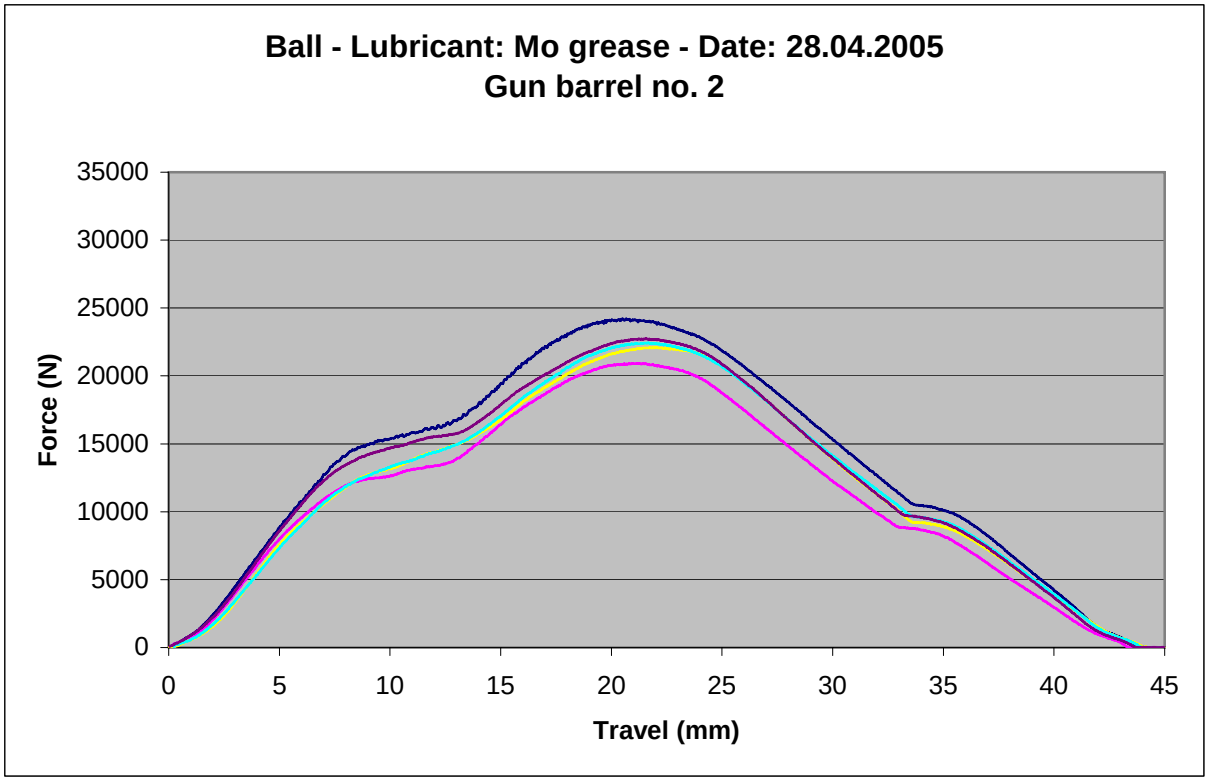


*Figure 8.2: The measured force as a function of the penetration distance.*

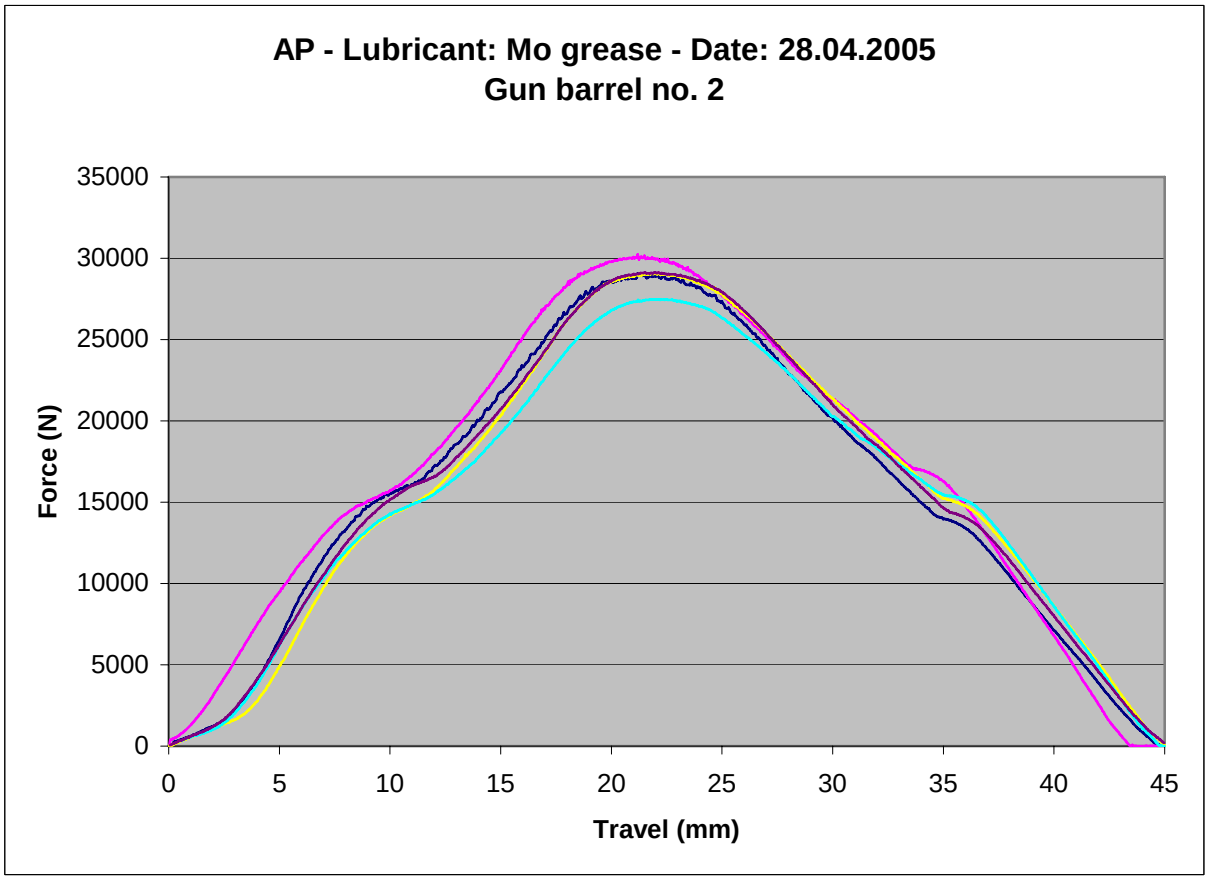


*Figure 8.3: The measured force as a function of the penetration distance.*

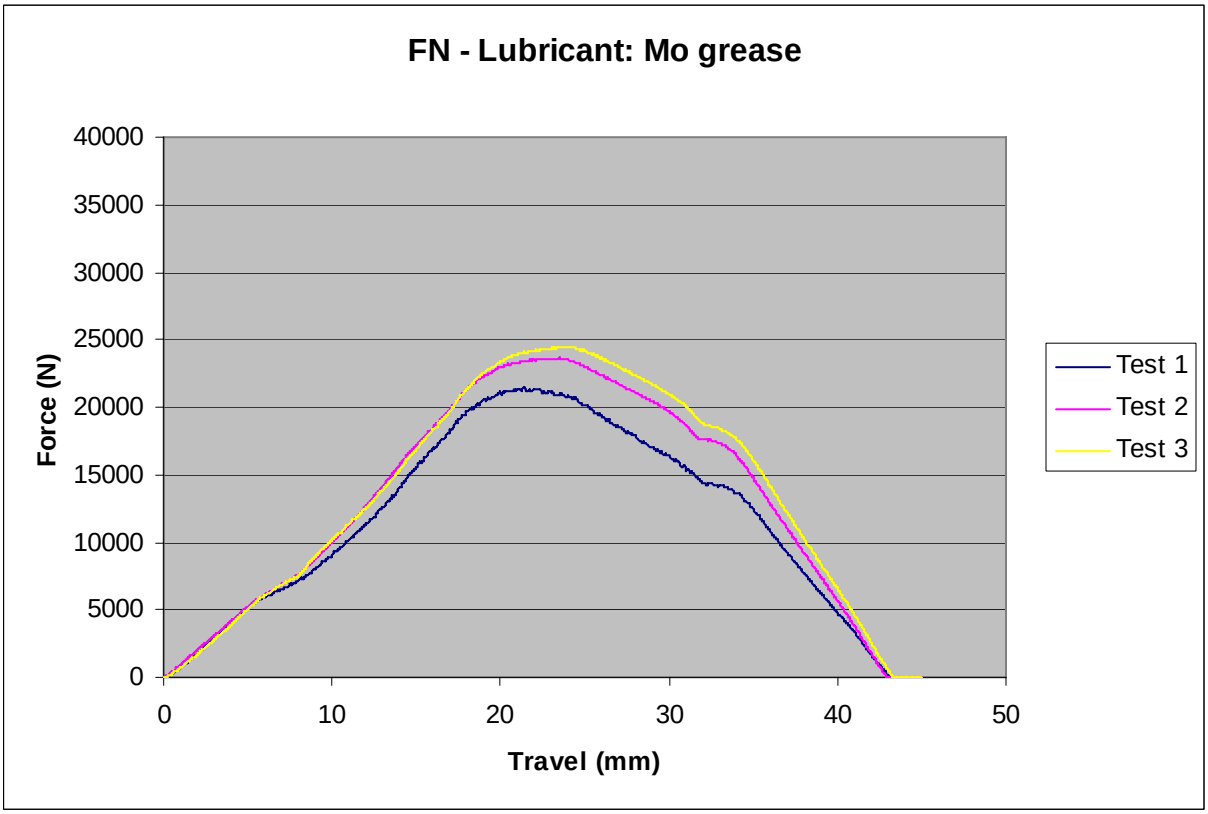


*Figure 8.4: The measured force as a function of the penetration distance.*

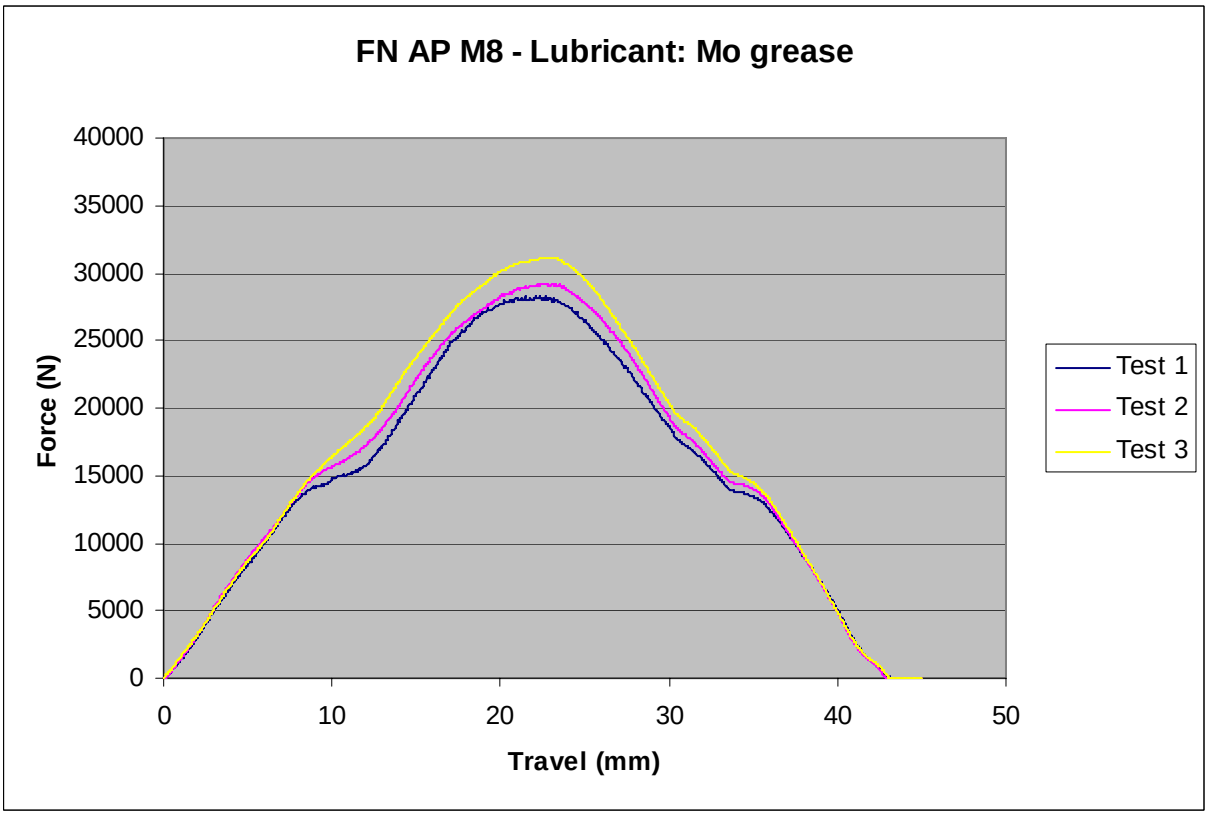


*Figure 8.5: The measured force as a function of the penetration distance.*

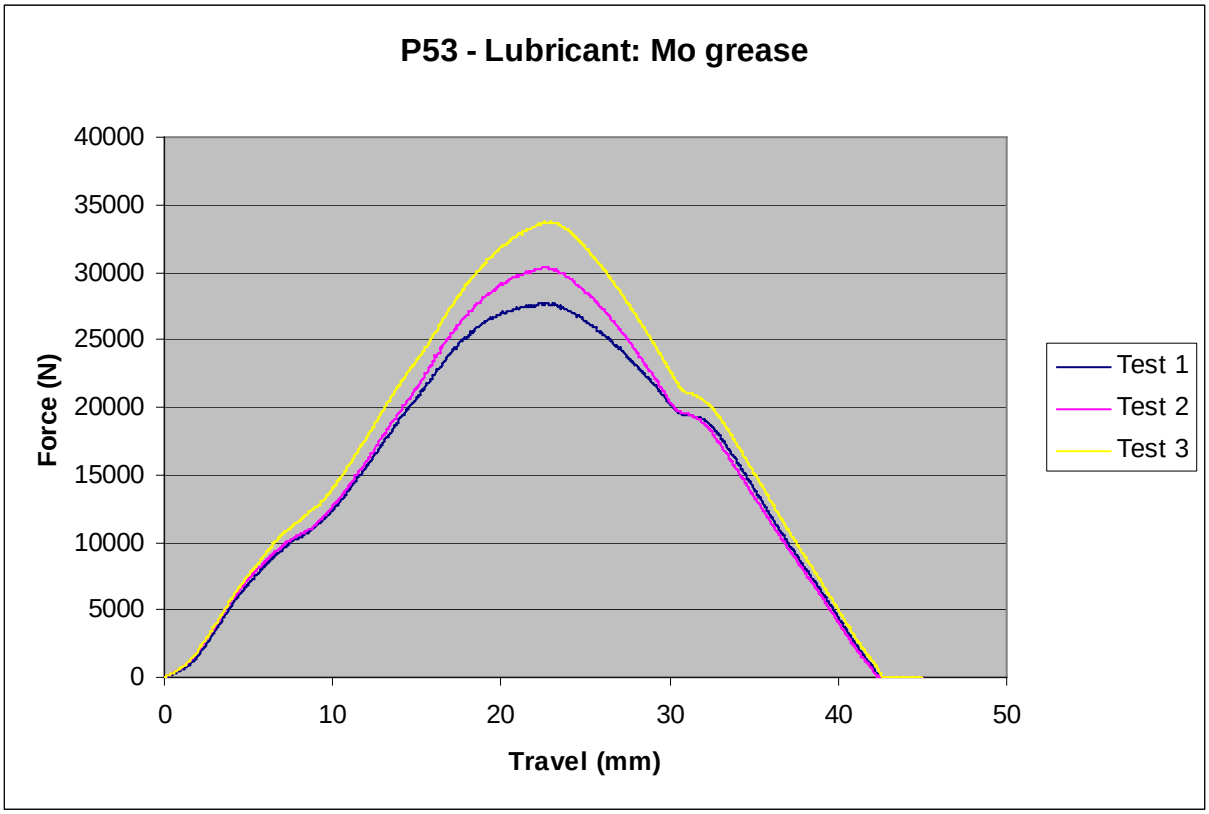


*Figure 8.6: The measured force as a function of the penetration distance.*

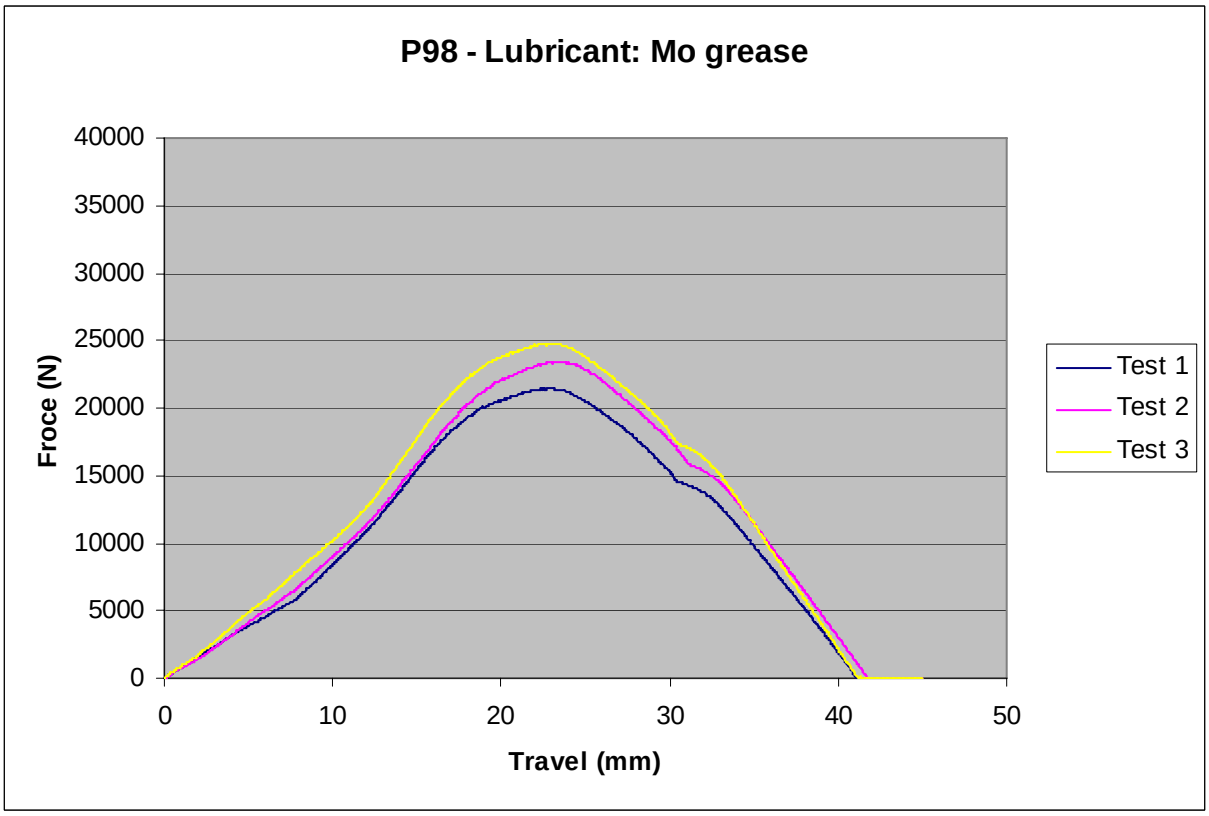


*Figure 8.7: The measured force as a function of the penetration distance.*

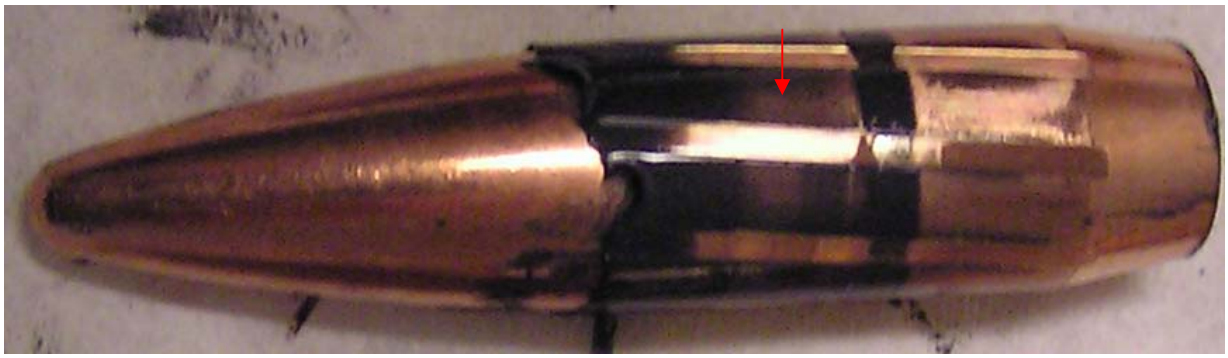

*Figure 8.8: FN*

*Figure 8.9: FN APM8*

*Figure 8.10: P53*

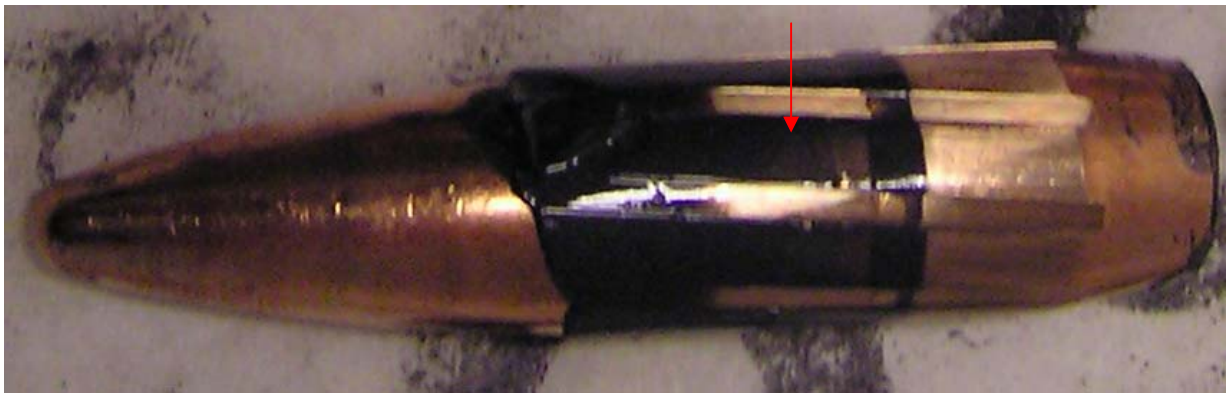

*Figure 8.11: P98*

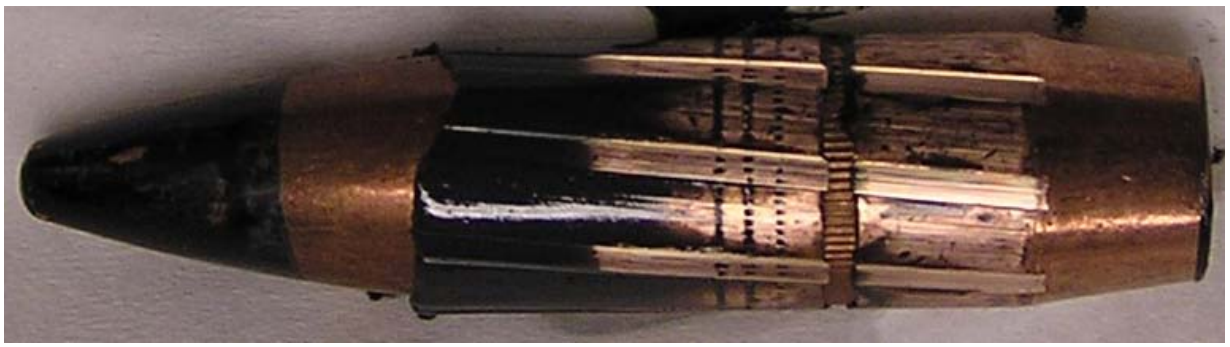

*Figure 8.12: AP*

*Figure 8.13: Ball*

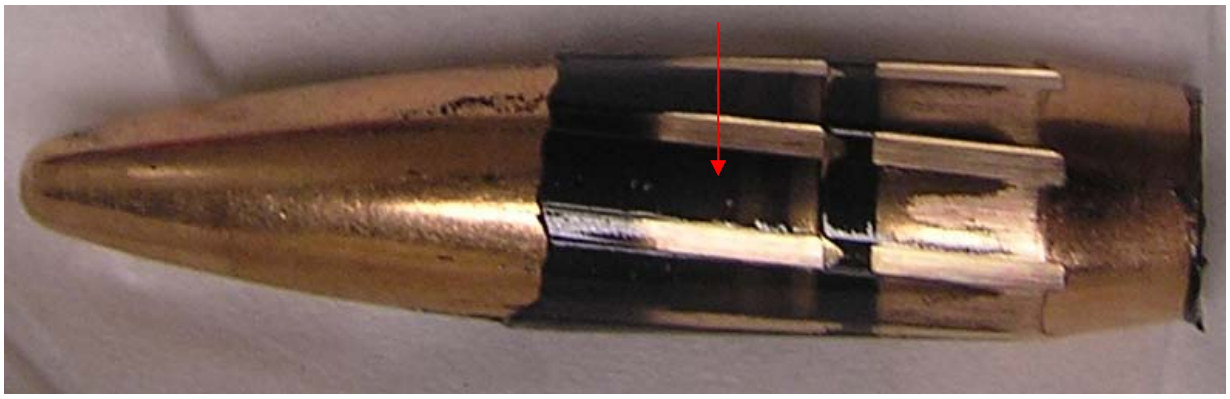

*Figure 8.14: MP-inert*

We find that the force necessary to press the projectiles into the gun barrel is larger for the AP projectiles. This seems reasonable since the hardcore will tend to decrease the inward compression of the projectile when entering into the grooves. This can lead to a larger normal stress and a larger normal friction force. It is well known from the shooting range that AP tends to increase the wear of gun barrels. The P 53 also seems to give a large friction force. The reason for this is that this projectile is more like an AP projectile with a hardened inner steel core.

| | MP inert | Ball | AP | FN | FNAPM8 | P53 | P98 |
|---|---|---|---|---|---|---|---|
| Core | Mild steel and WC | Mild steel | Hardened steel | Mild steel and WC | Hardened steel | Hardened steel | Mild steel and WC |
| Outer diameter | 12.96mm | 12.96mm | 12.96mm | 12.96mm | 12.96mm | 12.95mm | 12.96mm |
| Force | 21000N | 22500N | 27500N | 22500N | 28000N | 30000N | 22500N |

*Table 8.1: The maximum force necessary to press the projectile into the gun barrel.*

To further study the forces on the projectiles during in-pressing we studied the amount of grease left on the projectile after being pushed into the gun barrel. The grease was initially situated only in the gun barrel. For the projectiles with low in-pressing forces we found that the grease was situated along the surface of the projectile after impressing (arrows in figures 8.8-8.14). This suggests that the surface of the grooves of the gun barrel and the projectile were not in contact due to the inward bending of the projectile during penetration. When the hard cores of the projectiles were made of hardened steel, the inward bending is probably much smaller and the grease found on the projectile was much smaller. Thus we observe that the amount of grease found on the projectile anti-correlates with the in-pressing force.

## 9 CONCLUSION/DISCUSSION

The experimental results tell us

- The heat-affected region is near the surface of the lands.
- The lands are worn and rounded.
- Asymmetric wear and heat affected regions are observed.
- Cracks develop both in the heat affected region on the lands and in the grooves.
- We did not observe the white layer of cementite for the 25 shot structures but it was clearly seen on the worn-out barrel.
- Some residues of the gun barrel gases are found in the cracks.
- The heat-affected region is approximately a factor of 2 harder than the original material.
- AP projectiles are associated with larger forces to press the projectiles into the gun barrel.
- The amount of grease on the projectiles anti-correlate with the in-pressing force.

The asymmetric wear and the asymmetric heat affected region are probably related to the rotation of the projectile when entering into the gun barrel. The cracks probably develop due to thermal stress.

The theoretical calculations and the experimental results both suggest that the mechanical friction between the projectile and the gun barrel is a significant contributor to the heat-affected zone of the lands of the gun barrel for the first 25 shots for the 12.7mm MP round. The force necessary to only deform plastically the jacket of the projectile is a factor of 10 smaller. The literature reports that the wear per shot is constant unless large burst are performed.

So why do different gun barrel gases in general give different wear rates of gun barrels? In general the heat flux to the lands are given additively by the heat flux from the gun barrel gases and the heat flux from friction. [1]In general we believe that the large wear rate on the lands

[1] Although hypothetically assuming the heat flux from gun barrel gases could be smaller than the heat flux from friction,- this does not mean that the temperature and the composition of the gun barrel gases are insignificant. The reaction chemistry is dependent of the composition of the gun barrel gases, the temperature of the steel and the temperature of the gun barrel gasses. The maximum temperature of the gun barrel gases is in general around 3000K, while he maximum temperature of the steel is around 1500K. Thus reducing the temperature or the

observed for almost every gun barrel is due to a) higher temperature on the lands due to mechanical friction, and b) large mechanical wear on the lands due to mechanical friction These two mechanisms are related and could be changed by changing the

- The diameter of the projectile
- The friction coefficient between the jacked and the gun barrel
- The geometrical structure of the projectile
- The hardness of the steel casing inside the projectile.

In ongoing work the following specific question is addressed: What is the exact magnitude of the heat flux on the lands due to gun barrel gases and friction during a shot?

**Acknowledgment**
We thank Knut Kristensen and Knut Rørhus at Nammo for interesting discussions and for providing material samples for the study in this article.

**REFERENCES**

1. Lawton B., " Thermo-chemical Erosion in Gun Barrels", Wear 251 (2001) 827-838
2. Plett E.G., Alkidas A.C., Shrader R.E. and Summerfield M., " Erosion of Metals by High Pressure Combustion Gases: Inert and Reactive Erosion", Jour. of Heat Transfer, 110-115, Feb. 1975
3. Alkidas A.C., Morris S.O. and Summerfield M., " Erosive effects of High–Pressure Combustion Gases on Steel Alloys", Jour. Spacecraft, Vol.13, No.8, 461-465, Aug. 1976
4. Alkidas A.C., Christoe C.W., Caveny L.H. and Summerfield M." Erosive Effects of High Pressure and High Temperature Gases on Steel", Jour. of Engineering Materials and Technology, 239-243, July, 1977.
5. Gany A., Caveny L.H. and Summerfield M., " Aerothermochemistry of Metal Erosion by Hot Reactive Gases", Jour. of Heat Transfer, 531-536, Aug. 1978
6. Gany A., Caveny L.H. and Johnson J.W.," Water Vapor Contribution to the Erosion of steel by High Temperature Flows", Jour. of Heat Transfer, Vol. 103, May 383-386, 1981
7. Greaves R.H., Abram H.H. and Rees S.H.," Erosion of Guns", Jour. of Iron and Steel Institute", Vol. 117, 113-117, 1929
8. Evans R.C., Horn F.H., Shapiro Z.M. and Wagner R.L., " The Chemical Erosion of Steel by Hot Gases Under Pressure", Jour. of Phys. Col. Chemistry, Vol. 51,1404-1420, 1947
9. Rosenband V., Schneebaum Y. and Gany A., " Some thermodynamic aspects related to steel reactive erosion", Wear 221, 109-115, 1998
10. Gallier S., Bac J.P. and Pieta P.D., " Numerical Modelling of Chemical Erosion in Gun Tubes", "20 th International Symposium on Ballistics, Orleando,FL-23-27 Sept. 2002
11. Sopok S., Hara, P.O. ,Pfleg G., Dunn S., Coates D. And Nickerson G., " Unified Computer model for Predicting Thermochemical Erosion in Gun Barrels", Journ. Of Propulsion and Power, Vol. 15,No . 4, July-August , 601-612, 1999
12. Cote P.J., Todaro M.E., Kendall G. and Witherell M. ,"Gun bore erosion mechanisms revised with laser pulse heating", Surface and Coatings Technology 163-164 (2003) 478-483
13. Cote P.J., Todaro M.E., Kendall G. and Witherell M. ," Laser pulse heating of gun bore coatings ",Surface and Coatings Technology 146-147 (2001) 65-69
14. Cote P.J. and Rickard C. " Gas-metal reaction products in the erosion of chromium-plated gun bores", Wear 241 (2000) 17-25
15. Underwood J.H. " Letter to the editor", Wear 241 (2000) 118-119

---

composition of the gun barrel gases could change the reaction chemistry significantly while only marginally changing the temperature of the steel.

16. Botstein O. and Arone R., “ The micro structural changes in the surface layer of gun barrels”, Wear, 142 (1991) 87-95
17. Turley D.M., Cumming G. and McDermott I., “ A metallurgical study of erosive wear in a 105 mm tank gun barrel”, Wear, 176 (1994) 9-17

**APPENDIX A**

# Chemical composition M2 12.7 mm gun barrel

| *Elements* | *Atomic %* |
|---|---|
| **Iron** | 95.97 |
| **Carbon** | 0.411 |
| **Chromium** | 1.090 |
| **Manganese** | 0.915 |
| **Molybdenum** | 0.696 |
| **Silicon** | 0.292 |
| **Vanadium** | 0.216 |
| **Nickel** | 0.174 |
| **Copper** | 0.166 |
| **Others** | 0.057 |

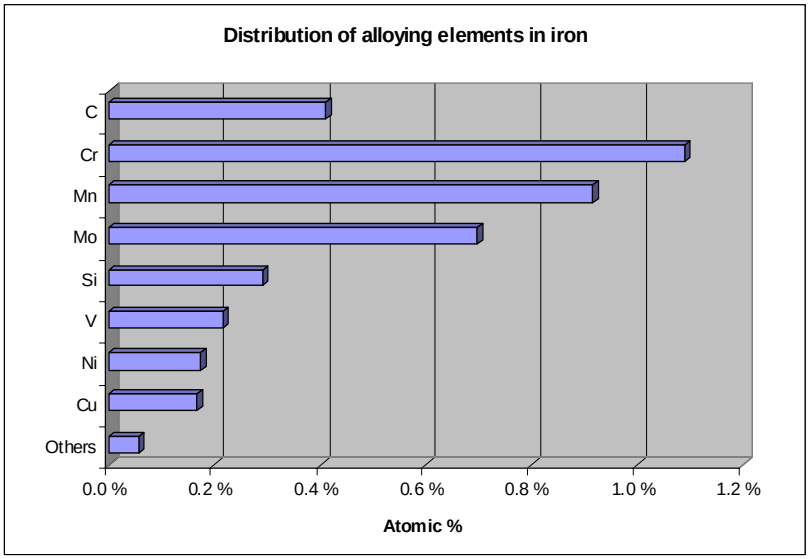


EPMA Run no. 1

| C | Fe | Cu | Total |
|---|---|---|---|
| 13.27 | 74.22 | 0.06 | 87.55 |
| 10.4 | 77.15 | 0 | 87.55 |
| 11.22 | 77.3 | 0.04 | 88.56 |
| 10.85 | 76.43 | 0.05 | 87.33 |
| 9.05 | 77.95 | 0.06 | 87.06 |
| 7.85 | 77.55 | 0.04 | 85.44 |
| 10.66 | 77.37 | 0.08 | 88.11 |
| 7.04 | 77.59 | 0.08 | 84.71 |
| 6.44 | 77.29 | 0.11 | 83.84 |
| 6.65 | 77.57 | 0 | 84.21 |
| 6.84 | 77.8 | -0.01 | 84.64 |
| 9.1 | 77.62 | 0.01 | 86.73 |
| 10.09 | 77.39 | 0.04 | 87.52 |
| 8.7 | 77.94 | 0.07 | 86.7 |
| 6.07 | 78.11 | 0.06 | 84.24 |
| 6.38 | 77.83 | 0.08 | 84.3 |
| 5.96 | 78.15 | 0.01 | 84.13 |
| 6.08 | 77.86 | 0.05 | 83.99 |
| 4.8 | 78.41 | 0.05 | 83.26 |
| 5.59 | 78.74 | 0.03 | 84.35 |
| 7.32 | 78.31 | 0.05 | 85.68 |

| | | | |
|---|---|---|---|
| 4.92 | 78.61 | 0.02 | 83.56 |
| 9.89 | 78.3 | 0.04 | 88.23 |
| 7.96 | 78.21 | 0.07 | 86.25 |
| 5.48 | 78.43 | 0.01 | 83.92 |
| 6.69 | 77.97 | 0.04 | 84.7 |
| 4.83 | 78.45 | 0.07 | 83.35 |
| 5.27 | 78.29 | 0.06 | 83.62 |
| 5.58 | 78.59 | 0.07 | 84.24 |
| 5.18 | 78.74 | 0.02 | 83.94 |
| 6.85 | 78.74 | 0.01 | 85.61 |
| 9.29 | 78.26 | 0.06 | 87.61 |
| 9.37 | 78.38 | 0.06 | 87.82 |
| 7.29 | 78.26 | 0.07 | 85.62 |
| 7.14 | 78.68 | 0.02 | 85.84 |
| 6.17 | 78.9 | 0 | 85.07 |
| 5.49 | 79.07 | 0.02 | 84.57 |
| 4.99 | 79.02 | 0.07 | 84.09 |
| 5.24 | 79.21 | 0.02 | 84.47 |
| 5.71 | 78.44 | 0.08 | 84.22 |
| 7.68 | 78.48 | 0.05 | 86.21 |
| 8.97 | 78.43 | 0.06 | 87.46 |
| 9.63 | 78.7 | 0.09 | 88.43 |
| 7.07 | 78.28 | 0.03 | 85.38 |
| 5.87 | 78.7 | 0.04 | 84.61 |
| 6.16 | 79.35 | 0.06 | 85.57 |

EPMA Run no. 2

| C | Fe | Cu | Total |
|---|---|---|---|
| 11.32 | 75.83 | 0.04 | 87.19 |
| 10.17 | 77.28 | 0.1 | 87.55 |
| 10.52 | 77.71 | -0.01 | 88.24 |
| 9.47 | 77.7 | 0.06 | 87.23 |
| 7.05 | 77.94 | 0.06 | 85.05 |
| 9.82 | 78.28 | 0.01 | 88.12 |
| 5.9 | 78.82 | 0.08 | 84.8 |
| 28.53 | 76.26 | 0.17 | 104.96 |
| 7.11 | 78.29 | -0.05 | 85.4 |
| 7.8 | 78.42 | 0.01 | 86.24 |
| 8.15 | 78.77 | 0.06 | 86.97 |
| 8.54 | 78.83 | 0.03 | 87.41 |
| 6.67 | 78.9 | 0.07 | 85.64 |
| 10.93 | 77.78 | 0.03 | 88.73 |
| 7.21 | 78.62 | 0.05 | 85.88 |
| 5.66 | 79.11 | 0.04 | 84.81 |
| 6.74 | 78.96 | 0.05 | 85.75 |
| 6.49 | 78.58 | 0 | 85.08 |
| 6.17 | 79.53 | 0.06 | 85.77 |
| 5.78 | 79.2 | 0.09 | 85.08 |
| 7.98 | 78.87 | 0.05 | 86.9 |
| 7.28 | 79.02 | 0.06 | 86.36 |
| 5.88 | 79.65 | 0.05 | 85.58 |
| 5.51 | 79.1 | 0.01 | 84.62 |
| 5.21 | 79.03 | -0.02 | 84.24 |

| | | | |
|---|---|---|---|
| 6.38 | 79.03 | 0.04 | 85.46 |
| 4.74 | 79.51 | 0.05 | 84.3 |
| 5.34 | 79.09 | 0.05 | 84.48 |
| 4.9 | 79.56 | 0.04 | 84.5 |
| 7.43 | 79.09 | 0.07 | 86.6 |
| 8.32 | 79.55 | 0.03 | 87.9 |
| 5.84 | 79.54 | 0.03 | 85.41 |
| 6.77 | 79.5 | 0.05 | 86.32 |
| 6.2 | 79.25 | 0.02 | 85.47 |
| 5.09 | 79.4 | 0.09 | 84.57 |
| 5.8 | 79.34 | 0.04 | 85.17 |
| 5.84 | 80.01 | 0.02 | 85.88 |
| 5.11 | 79.91 | 0.02 | 85.03 |
| 6.9 | 80.17 | 0.02 | 87.09 |
| 8.04 | 79.91 | 0.11 | 88.06 |
| 8.41 | 80.03 | 0.03 | 88.47 |
| 6.27 | 79.73 | 0.04 | 86.04 |
| 5.84 | 79.99 | 0.06 | 85.89 |
| 6.13 | 80.32 | 0.06 | 86.51 |

EPMA Run no. 3

| C | Fe | Cu | Total |
|---|---|---|---|
| 17.16 | 55.41 | 2.26 | 74.83 |
| 6.37 | 77.74 | 0.15 | 84.26 |
| 7.49 | 78.28 | 0.03 | 85.8 |
| 6.07 | 79 | 0.06 | 85.12 |
| 5.46 | 78.91 | 0.05 | 84.42 |
| 6.52 | 79.61 | 0.12 | 86.25 |
| 8.75 | 79.38 | 0.01 | 88.15 |
| 7.89 | 79.39 | 0.06 | 87.34 |
| 7.89 | 79.27 | 0 | 87.16 |
| 5.59 | 79.65 | 0.02 | 85.25 |
| 6.07 | 79.88 | -0.01 | 85.94 |
| 5.58 | 79.92 | 0.06 | 85.55 |
| 6.07 | 79.44 | 0.02 | 85.54 |
| 4.56 | 80.04 | 0.04 | 84.64 |
| 5.85 | 79.04 | 0.09 | 84.98 |
| 6.69 | 79.43 | 0.1 | 86.21 |
| 4.72 | 79.77 | 0.07 | 84.57 |
| 7.5 | 79.87 | 0.04 | 87.41 |
| 6.5 | 79.53 | 0.06 | 86.09 |
| 6 | 80.05 | -0.01 | 86.06 |
| 5.24 | 79.79 | 0.09 | 85.11 |
| 4.75 | 80.34 | 0.04 | 85.14 |
| 5.16 | 80.38 | 0.03 | 85.57 |
| 5.39 | 80.47 | 0.06 | 85.93 |
| 4.77 | 80.51 | 0.03 | 85.3 |
| 6.44 | 80.59 | 0.09 | 87.12 |
| 7.44 | 80.23 | 0.05 | 87.72 |
| 8.07 | 80.07 | 0.12 | 88.26 |
| 6.66 | 80.65 | 0.04 | 87.35 |
| 6.05 | 80.42 | 0.07 | 86.53 |
| 4.88 | 80.39 | 0.06 | 85.33 |
| 5.11 | 80.41 | 0.06 | 85.58 |
| 7.43 | 79.47 | 0.02 | 86.93 |
| 5.44 | 80.74 | 0.01 | 86.19 |
| 5.45 | 80.09 | 0.02 | 85.55 |
| 6.79 | 80.24 | 0.07 | 87.1 |
| 8.02 | 80.6 | 0.09 | 88.7 |
| 7.76 | 80.67 | 0.07 | 88.5 |
| 6.91 | 80.19 | 0.08 | 87.18 |
| 6.85 | 80.79 | 0.07 | 87.71 |
| 6.02 | 80.34 | 0 | 86.36 |

X-ray image of 12,7 mm MP inert projectiles